An Integrated YOLOv7–Fuzzy Reasoning Framework for Interpretable and Robust Cantaloupe (Cucumis melo) Growth-Stage Assessment

Sikudhan Lucas Mpuhus
University of Technology Malaysia
Mohamad Shukri Zainal Abidin
shukri@utm.my
University of Technology Malaysia
Mohd Shahkhirat bin Norizan
Bandar Pusat Jengka Pahang
Muhammad Shahrul Azwan bin Ramli
University of Technology Malaysia
Keshinro Kazeem Kolawole
University of Technology Malaysia
Rizqi Andry Ardiansyah
University of Technology Malaysia
Kasirye Joshua
University of Technology Malaysia

Research Article

Keywords: Deep neural network, Fuzzy logic, Growth detection, Rock melon (cantaloupe), YOLOv7

Posted Date: February 18th, 2026

DOI: https://doi.org/10.21203/rs.3.rs-8600877/v1

Additional Declarations: No competing interests reported.

An Integrated YOLOv7–Fuzzy Reasoning Framework for Interpretable and Robust Cantaloupe (Cucumis melo) Growth-Stage Assessment

Sikudhan Lucas Mpuhus[1,2], Mohamad Shukri Zainal Abidin[1], Mohd Shahkhirat bin Norizan[3], Muhammad Shahrul Azwan bin Ramli[4], Keshinro Kazeem Kolawole[1], Rizqi Andry Ardiansyah[1], Kasirye Joshua[1]

1 Division of Control and Mechatronics Engineering, Faculty of Electrical Engineering, Universiti Teknologi Malaysia, (UTM) Skudai - Johor, Malaysia.
2 Mbeya university of Science and technology, Mechanical and industrial department,P.O.Box 131, 53119 Mbeya-Tanzania.
3 Agronomy Department FGV R&D Sdn Bhd PPP Tun Razak 26400 Bandar Pusat Jengka Pahang, Malaysia.
4 Petronas Research Sdn. Bhd, Bangi- Selangor, Malaysia.

[*]Corresponding author: Dr Mohamad Shukri Zainal Abidin Tel: +60178866840
Email Address: shukri@utm.my

Highlights

1. A hybrid YOLOv7–fuzzy reasoning framework is proposed to transform raw object detections into interpretable, decision-level assessments of cantaloupe growth conditions.
2. Longitudinal detection data from multiple cultivation cycles were analyzed to derive canonical, season-invariant growth patterns that form the basis of an expert-informed fuzzy knowledge base.
3. The fuzzy reasoning layer integrates temporal context and agronomic rules to stabilize growth-stage interpretation under detection uncertainty and class imbalance.
4. An ablation study demonstrates that fuzzy reasoning enhances decision robustness and interpretability without altering or degrading object detection performance.
5. Real-world deployment on edge hardware confirms the system's ability to generate actionable, confidence-aware crop condition alerts for greenhouse precision farming.

Impact

This work advances precision agriculture by moving beyond frame-level object detection toward decision-oriented crop assessment, enabling interpretable, confidence-aware growth monitoring under real greenhouse conditions. By integrating deep learning perception with agronomic fuzzy reasoning, the proposed framework supports timely, knowledge-driven interventions that align with the core principles of precision agriculture: targeted management, reduced uncertainty, and data-informed decision making.

Abstract

Background: Precision agriculture increasingly relies on computer vision systems to monitor crop growth; however, most existing approaches remain limited to frame-level object detection and do not support agronomic decision-making under uncertainty. To address this limitation, this study develops an interpretable and robust framework for cantaloupe (*Cucumis melo*) growth-stage assessment by integrating deep learning–based visual perception with fuzzy reasoning.

Results: A YOLOv7 detector was fine-tuned to identify healthy leaves, wilted leaves, flowers, and fruits from greenhouse imagery collected across eleven cultivation cycles at three production sites. The detected class counts were temporally aggregated and used as inputs to a Mamdani-type fuzzy inference system encoding expert agronomic knowledge and growth-stage expectations. Experimental evaluation showed that YOLOv7 achieved the highest mAP@0.5 (0.771) and balanced precision–recall performance compared with other YOLO variants, while the fuzzy reasoning layer transformed noisy object-level outputs into consistent crop-condition states with associated confidence levels. Real-world deployment on an edge device further demonstrated the system's ability to generate actionable alerts, such as "Check Flower" and "Abnormal Condition," aligned with expected phenological trends.

Conclusions: The proposed framework advances beyond conventional detection pipelines by enabling decision-level crop assessment that is interpretable, temporally aware, and robust to visual uncertainty. This approach provides a practical decision-support tool for greenhouse crop monitoring and supports the broader adoption of intelligent, confidence-aware systems in precision agriculture.

Keywords: Deep neural network; Fuzzy logic; Growth detection; Rock melon (cantaloupe); YOLOv7

1 Introduction

The global shift toward precision agriculture has accelerated the adoption of advanced sensing, computer vision, and data-driven decision-support systems to improve crop productivity and sustainability (1–5). In fruit cultivation, these technologies play a critical role in crop monitoring, disease surveillance, yield estimation, and growth condition assessment, directly influencing per-acre productivity, harvesting strategies, and supply-chain management (6,7,16–25,8–15) . Accurate and timely assessment of plant growth dynamics is therefore essential not only for maximizing yield but also for reducing labor costs and minimizing resource wastage.

Recent advances in deep neural networks (DNNs) have significantly enhanced the ability to extract both low-level and high-level semantic features from complex agricultural scenes (20,25,34–41,26–33). These capabilities have enabled vision-based systems to move beyond simple visual inspection toward automated, large-scale monitoring of plant health and development. However, real-world agricultural environments remain highly challenging for vision-based detection systems due to illumination variability, occlusion from leaves and branches, fruit overlap, and complex background textures (19,22,48,26,27,42–47). Such factors often degrade detection reliability, particularly during early growth stages when visual cues are subtle. Consequently, robust algorithms that can tolerate visual uncertainty while maintaining real-time performance are urgently needed (20,21,49).

Deep learning–based object detection frameworks are generally categorized into single-stage and two-stage architectures. Two-stage detectors, such as Faster R-CNN, CenterNet2, and Variable Filter Networks, rely on region proposal mechanisms followed by classification, offering high accuracy but often at the expense of computational efficiency (14,22,24,42,45,50). In contrast, single-stage detectors—most notably the YOLO (You Only Look Once) family—formulate detection as a unified regression problem that simultaneously performs localization and classification, eliminating the need for region proposal networks (14,15,23,43,50). This architectural simplicity enables faster inference and makes YOLO-based models particularly suitable for deployment in embedded and edge-computing agricultural systems (5,12,16,17,51–53).

Among the YOLO variants, YOLOv7 has demonstrated strong performance in balancing detection accuracy and computational efficiency, making it an attractive candidate for real-time agricultural applications. Nevertheless, YOLO-based detectors alone provide discrete detection outputs that may fluctuate across time due to noise, class imbalance, and environmental variability (14,37,39,45,48,54,55). While such outputs are valuable for object-level recognition, they are insufficient for higher-level agronomic decision-making, which inherently involves uncertainty, temporal dependencies, and expert knowledge.

To address these limitations, fuzzy logic has been widely adopted as a complementary reasoning framework capable of modeling uncertainty and imprecision in complex systems (56–60) . In agricultural applications, fuzzy logic has proven effective in decision support, automatic control, and vision-based pest and disease management, where crisp thresholds fail to capture gradual transitions in plant conditions (56,59–63). Integrating deep learning perception with fuzzy reasoning offers a principled pathway to transform noisy visual detections into stable, interpretable, and actionable agronomic assessments. The efficacy of this hybrid perception-reasoning framework were demonstrated in the context of cantaloupe (Cucumis melo) growth monitoring, a high-value crop where continuous developmental assessment is critically needed.

This study focuses on cantaloupe (*Cucumis melo*, commonly known as rockmelon in Southeast Asia), specifically the Glamour cultivar (commercially designated as Melon Manis Terengganu or Golden Langkawi), which belongs to the inodorus botanical group (64–66) Cantaloupe is a high-value crop cultivated extensively across temperate and tropical regions, with China leading global production at over 31 million tons annually, followed by Turkey, Iran, the United States, and several Mediterranean and Asian countries (65) . Malaysia presents favorable climatic conditions for cantaloupe cultivation, with optimal growth temperatures ranging from 18 °C to 30 °C. Major production regions include Kelantan, Kedah, Terengganu, Selangor, and Johor, where Kelantan alone accounts for over 347 hectares of cultivation area (64–68).

Despite its economic importance, effective monitoring of cantaloupe growth from vegetative stages through flowering and fruiting remains labor-intensive and costly (58). Existing studies predominantly focus on detecting mature fruits or a limited number of growth stages, emphasizing final yield quality rather than continuous plant development (13–15,69–71). This narrow scope restricts farmers' ability to diagnose early stress conditions, identify causes of yield reduction, and take timely corrective actions. Furthermore, most vision-based approaches lack temporal interpretation and fail to provide intuitive visual summaries of plant growth trends, which are essential for practical farm-level decision-making (12,15,18).

To bridge these gaps, this work proposes an integrated YOLOv7–fuzzy reasoning framework for comprehensive cantaloupe growth analysis across multiple developmental stages. YOLOv7 is first fine-tuned to detect key agronomic indicators healthy leaves, wilted leaves, flowers, and fruits under real greenhouse conditions. The resulting detection outputs are aggregated over time and combined with cultivation-stage information to form an agronomic feature vector. A Mamdani-type fuzzy inference system then translates these features into interpretable crop condition assessments, enabling robust decision-level reasoning under uncertainty. While recent studies have demonstrated the effectiveness of YOLO-based detectors for fruit and leaf recognition, most approaches terminate at object-level detection and rely on farmers to interpret results manually. Such systems do not explicitly address temporal growth behavior, class imbalance, or decision uncertainty, which are critical in real greenhouse environments. This study addresses these limitations by integrating YOLOv7 with a fuzzy reasoning layer that operates at the decision level, transforming noisy multi-class detections into interpretable, growth-aware agronomic assessments. The main contributions of this study are threefold:

I. The development of a multi-stage cantaloupe growth monitoring system based on YOLOv7 that extends beyond fruit-only detection;

II. The integration of fuzzy reasoning to stabilize deep learning outputs and provide interpretable crop condition assessments across cultivation stages; and

III. A comprehensive experimental evaluation comparing the proposed framework against multiple YOLO variants using precision, recall, F1-score, mean average precision (mAP), and temporal growth trend analysis.

By unifying deep visual perception with fuzzy decision-making, the proposed approach offers a practical and scalable solution for intelligent crop monitoring, supporting farmers with actionable insights to improve yield quality, reduce monitoring costs, and enhance overall farm productivity. However, the framework does not yet incorporate environmental variables or multi-cultivar validation, which remain directions for future study.

2 Methods

2.1 Cultivation of the cantaloupe plant

The cantaloupe (Cucumis melo) plants used in this study were grown from commercial seeds of the ‘Glamour F1 Hybrid’ variety (supplied by Sakata Seed Corporation, Yokohama, Japan). The seeds were purchased in Malaysia through the authorized agricultural distributor CNC Marketing (72). No wild, collected, gifted, or genetically modified plant materials were used.

Cultivation began in November 2023 by planting the seeds in peat moss-filled trays. The trays were covered with black plastic to protect the emerging leaves until the seedlings had 2-3 leaves. A total of 100 seeds were planted, and 59 plants grew to the harvesting stage, with one not bearing any fruit. After transplantation, leaf growth increased, and tendrils began climbing, supported by strings for vertical growth. By November 17, 2023, during the flowering stage, male flowers bloomed in the first week, followed by female flowers in the second week, as shown in Fig. 1. Manual pollination was performed in the mornings of the second week, transferring pollen from male to female flowers. Excess vines were trimmed to direct nutrients to the fruits and control growth. The fruiting period started on December 1, 2023. Fruits grew and developed netting on their surface. Wilting leaves indicated readiness for harvesting.

The plants were cultivated and monitored in three controlled greenhouse locations in Malaysia. Image data were collected from: (i) Universiti Teknologi Malaysia (UTM Green House): 1°33'30.3336" N, 103°37'33.4596" E (Skudai, Johor); (ii) Tun Abdul Razak Agriculture Research Center (Jengka GH1 and GH2): 3°52′59.1″ N, 102°31′59.5″ E (Jengka, Pahang); and

(iii) Community Farmhouse (Putrajaya1 & 2): 2°57′14.92″ N, 101°43′36.38″ E (Putrajaya). All plants were cultivated on-site under standard greenhouse management practices, and no external plant samples were transported between locations.

Fig. 1 Cantaloupe (Cucumis melo) flower morphology. (A) Male flower with prominent stamen. (B) Female flower with visible inferior ovary at the base

2.2 Image acquisition/capturing

A multi-source imaging strategy was employed to capture cantaloupe growth under varied agronomic and environmental conditions. Data collection spanned three geographically distinct production sites: the UTM research greenhouse (1°33'30.3336" N, 103°37'33.4596" E), and two commercial farms, Jengka GH1 and Jengka GH2, as detailed in Section 2.4. This approach ensured the dataset encompassed a wide range of illumination (morning, afternoon, bright sun), plant densities, occlusion levels, and background clutter, thereby enhancing model robustness. Two complementary acquisition methods were used. First, for the development and evaluation of the YOLO-based detection models, high-resolution images (3456 × 4608 pixels) were systematically captured at the UTM greenhouse using an HONOR X9a mobile phone (model RMO-NX1) (44). A total of 2,626 images were collected on a weekly basis from November 2023 to January 2024, between 8:00 AM and 2:30 PM. The camera was positioned at distances of 0.2 to 3.0 meters with angles varying from 30° to 85° to simulate diverse viewpoints. Second, to support the development and validation of the temporal fuzzy reasoning system, longitudinal image streams were acquired from fixed stationary cameras (espcam OV2640) installed at all three sites. These cameras captured daily images across multiple growing seasons, as summarized in Table 1. From these continuous streams, 785 representative weekly images were systematically sampled to form the development dataset for the fuzzy logic controller. This separation of data sources targeted weekly captures for object detection training and longitudinal daily captures for decision-layer development ensured a rigorous evaluation framework that decouples perception learning from higher-level agronomic reasoning.

2.3 Annotation and labelling

A total of 2626 images were captured at different growth stages, such as post-transplantation leaves, flowering, and fruiting. Manual labeling of cantaloupe targets was performed using LabelImg software to outline each stage with minimum bounding rectangles (19). The images were classified into healthy leaf, wilted leaf, flower, and fruit categories as shown in Fig. 2. Annotations were saved in YOLO format.

Fig. 2 Representative image annotation examples,manually drawn bounding boxes in LabelImg software identify and classify key cantaloupe growth structures: healthy leaf (green), wilted leaf (orange), flower (blue), and fruit (red)

2.4 Dataset size and distribution

The dataset used in this study was collected from three geographically and operationally distinct cantaloupe production sites, enabling the model to learn under heterogeneous cultivation conditions and improving generalization across environments. The first site, the UTM Greenhouse, is located at coordinates (1°33′30.3336″ N, 103°37′33.4596″ E) and is dedicated to controlled-environment cantaloupe cultivation across multiple growing seasons. This greenhouse is equipped with fixed surveillance cameras originally deployed for growth monitoring and operational security. Images are automatically captured on a daily basis between 10:00 AM and 3:00 PM and uploaded to a cloud-based storage system. Depending on seasonal research demands, either a single camera or up to four cameras are active concurrently. These cameras are identified as Camera @ C00 (07, 10, 11, and 12), also referred to as SPARE UTM (RPI-1).

The second data acquisition site, Jengka GH1, is a commercial cantaloupe farm located in Pahang at coordinates (3°52′59.1″ N, 102°31′59.5″ E). This facility operates three cultivation cycles per year and is similarly equipped with a camera-based monitoring system for both agronomic observation and security. Image acquisition at this site spans a longer daily window, from 7:00 AM to 6:00 PM, reflecting more diverse illumination conditions compared to the greenhouse environment. Six cameras, labeled GH1 Camera @ C00 (19–24), were deployed across the facility, capturing spatially varied views of plant development.

The third site, Jengka GH2, is another cantaloupe-producing farm in Pahang that mirrors the operational structure of Jengka GH1, including three cultivation cycles per year and daily image acquisition between 7:00 AM and 6:00 PM. This site is equipped with six cameras labeled C00 (25–30). The inclusion of Jengka GH1 and GH2 introduces substantial variability in background clutter, plant spacing, illumination, and growth dynamics, which is critical for evaluating the robustness of deep learning models under real-world agricultural conditions. Collectively, these three sites provide a diverse and longitudinal dataset that captures intra- and inter-seasonal variations in cantaloupe growth, forming a strong foundation for both deep learning–based detection and rule-based fuzzy reasoning.

2.5 Data Splits and Usage

To ensure methodological rigor and to avoid data leakage between learning and decision-making stages, the collected dataset was partitioned into two distinct subsets, each serving a specific purpose within the proposed framework: (i) training, validation, and testing of the YOLO-based detection models, and (ii) development of the fuzzy logic reasoning system. This separation ensures that object detection learning and decision-level reasoning are evaluated independently, strengthening the validity and generalizability of the proposed framework.

2.5.1 Data for YOLO Model Training, Validation, and Testing

The dataset used for training, validation, and testing of the YOLO models was exclusively sourced from the UTM Greenhouse to maintain a controlled learning environment and consistent annotation quality. Images were captured using HONOR X9a mobile phone, resulting in a total of 2,626 labeled images. This dataset was annotated into four object classes healthy leaf, wilt leaf, flower, and fruit representing key phenological and health indicators of cantaloupe plants.

The labeled data were partitioned following a standard supervised learning protocol, with 80% (2,100 images) allocated for training, 10% (263 images) for validation, and 10% (263 images) for testing. This split balances model optimization and unbiased performance evaluation while minimizing overfitting. Importantly, restricting YOLO training to a single site allows the subsequent evaluation of the fuzzy reasoning system on multi-site data, thereby decoupling perception learning from decision inference and strengthening the experimental design.

2.5.2 Data for Fuzzy Logic System Development

The fuzzy logic controller was developed using longitudinal data sampled across multiple cultivation cycles and locations, reflecting the temporal nature of crop growth assessment. For each cultivation season, up to seven images per week were randomly selected to represent weekly plant development, ensuring temporal continuity while controlling data redundancy. In total, eleven cultivation seasons were considered across the three sites. At the UTM Greenhouse, five cultivation cycles were recorded: March–May 2021 (A), October–December 2021 (B), March–June 2022 (C), March–May 2023 (D), and October 2023–January 2024 (E). Jengka GH1 contributed three cycles: October 2022–January 2023 (F), February–April 2023 (G), and May–August 2023 (H). Similarly, Jengka GH2 provided three cycles: October–December 2022 (I), January–April 2023 (J), and June–August 2023 (K).

These cycles collectively span different environmental conditions, cultivation practices, and growth dynamics. As summarized in Table 1, a total of 785 images were used for fuzzy logic system development. Unlike the YOLO training dataset, these images were not used for model learning but instead for aggregating class-wise detection counts over time. This design allows the fuzzy system to operate on higher-level agronomic indicators rather than raw images, enabling robust decision-making despite detection noise, class imbalance, and seasonal variability. The separation of perception (YOLO) and reasoning (fuzzy logic) data sources further reinforces the interpretability and generalization capability of the proposed framework.

Table 1 Data for developing the fuzzy logic system

Weeks	UTM Green House (UTM)					Jengka GH1			Jengka GH2		
	A	B	C	D	E	F	G	H	I	J	K
1	7	7	7	7	7	7	7	7	7	7	7
2	7	7	7	7	7	7	7	7	7	7	7
3	7	7	6	7	7	6	7	7	7	7	7
4	7	7	5	7	7	7	7	7	7	7	0
5	7	6	5	6	7	0	7	7	7	7	7
6	7	7	6	7	7	7	7	7	5	7	7
7	7	7	7	7	7	7	7	0	0	7	7

Weeks	UTM Green House (UTM)					Jengka GH1			Jengka GH2		
	A	B	C	D	E	F	G	H	I	J	K
8	7	7	7	7	7	7	7	0	2	7	7
9	7	7	7	7	7	7	7	0	7	7	7
10	7	7	7	7	7	7	7	0	7	7	0
11	7	7	7	4	7	7	0	0	7	7	0
12	7	3	7	0	7	3	0	0	0	7	0
Sub total	84	79	78	73	84	72	70	42	63	84	56
Grand total						785					

2.6 Class Distribution and Imbalance Analysis

An analysis of the final annotated dataset reveals a significant class imbalance, a common characteristic in agricultural datasets that reflects natural plant growth dynamics. As summarized in Table 2, vegetative structures healthy and wilted leaves dominate the dataset with 15,750 and 15,567 annotations, respectively. Reproductive organs, flowers and fruits, are less frequent, with 9,119 and 5,979 annotations. This distribution aligns with biological reality, as leaves are present throughout the growth cycle, while flowers and fruits appear only during specific, shorter phenological stages. Such imbalance is inherent to cantaloupe phenology, as vegetative structures persist throughout the growth cycle while reproductive organs appear only during limited stages. Although deep detectors can learn discriminative features under imbalance, detection outputs for minority but agronomically critical classes (flowers and fruits) remain more uncertain and temporally inconsistent. This limitation motivates the introduction of fuzzy reasoning in the proposed framework, which explicitly incorporates agronomic context and temporal relationships to mitigate uncertainty without modifying detector training

Table 2 Distribution of annotated instances for each class (healthy leaf, wilt leaf, flower, fruit) across the training, validation, and test datasets.

Class	Train	Validation	Test	Total
Healthy leaf	12,054	1,980	1,716	15,750
Wilt leaf	12,747	1,411	1,409	15,567
Flower	6,762	1,088	1,269	9,119
Fruit	4,807	679	493	5,979
Total	36,370	5,158	4,887	46,415

2.7 YOLOv7–Fuzzy Reasoning Integrated Architecture

The proposed system adopts a hybrid architecture that integrates a deep learning–based object detection model (YOLOv7) with a rule-based fuzzy inference system to achieve interpretable and temporally aware crop condition assessment as shown in Fig. 3. Initially, images are automatically acquired from fixed greenhouse cameras and undergo basic pre-processing, including resizing and normalization, to ensure compatibility with the YOLOv7 input resolution.

The YOLOv7 model is trained offline using annotated images to detect four agronomically relevant classes: healthy leaf, wilt leaf, flower, and fruit. Once trained, the model is deployed for inference, where it performs bounding box prediction, class assignment, and confidence filtering using non-maximum suppression. Rather than relying solely on pixel-level predictions, the system aggregates detection outputs by counting the number of detected objects per class over time, thereby converting low-level visual detections into meaningful agronomic indicators. To incorporate temporal crop development information, the system computes a growth-time index based on the week of cultivation, derived from the planting start date and the current observation date. The class-wise object counts and the growth-time index together form a crisp agronomic feature vector that characterizes the current crop state. These crisp inputs are then passed to a fuzzy logic module, where each variable is fuzzified using expert-defined membership functions representing linguistic terms such as low, medium, and high for leaf health, wilt severity, flower abundance, fruit load, and crop growth stage.

A Mamdani-type fuzzy inference engine processes these fuzzy inputs using a comprehensive expert rule base derived from agronomic knowledge of cantaloupe growth behavior across different cultivation stages. The fuzzy inference engine produces a fuzzy output representing the overall crop condition, which is subsequently defuzzified into a single interpretable crop condition index. This output is mapped to actionable decision categories, including normal condition, check wilt leaf, check flower, check fruit, and abnormal condition, along with an associated confidence level. Unlike conventional object detection systems that terminate at bounding box prediction, the proposed architecture extends detection results into a higher-level decision-making layer, enabling explainable and context-aware crop assessment. Finally, the detection results, annotated images, temporal trends, and fuzzy decision outputs are transmitted to a remote server for visualization and monitoring, allowing growers to track crop development and health status over time. This integration of YOLOv7 with fuzzy reasoning enhances robustness, interpretability, and suitability for real-world precision agriculture applications.

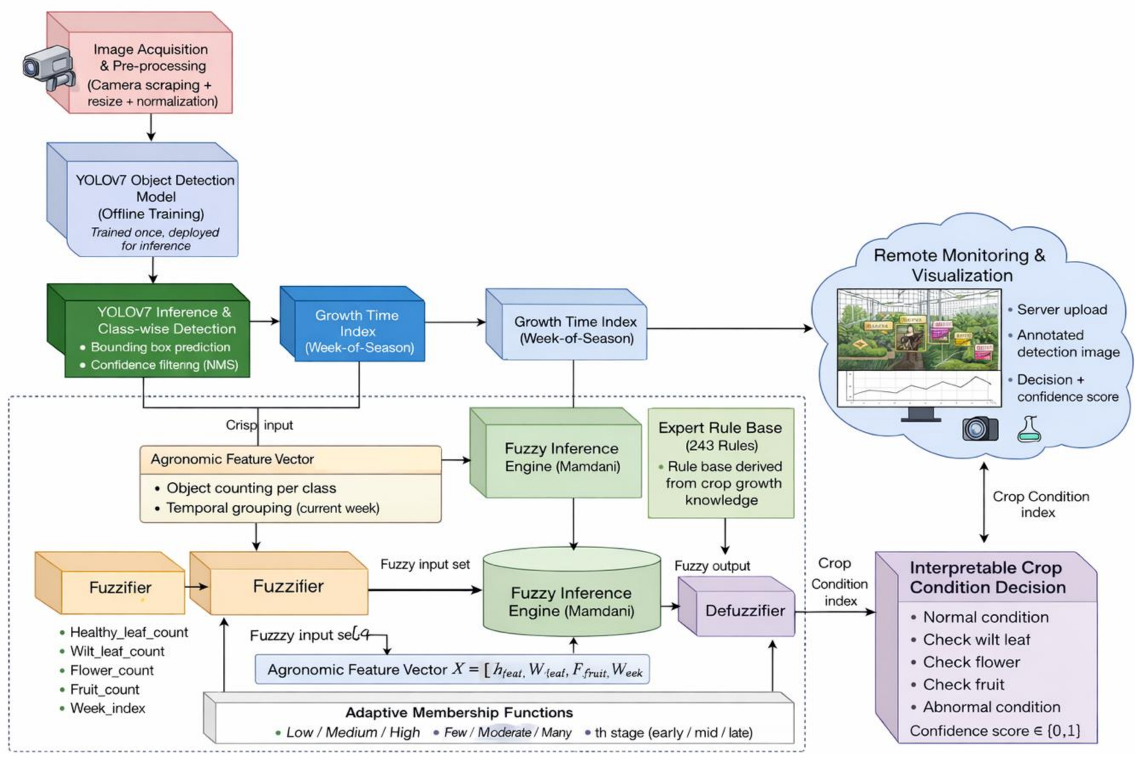

Fig. 3 The proposed architecture integrates YOLOv7-based visual perception with a fuzzy reasoning decision layer for crop condition assessment. Greenhouse images are automatically acquired and processed by a pretrained YOLOv7 detector to identify key agronomic indicators, including healthy leaves, wilted leaves, flowers, and fruits. Detected objects are aggregated into class-wise counts and combined with a temporal growth index (week-of-season) to form an agronomic feature vector. These features are mapped into fuzzy membership functions and evaluated using an expert-defined rule base within a Mamdani fuzzy inference system. The defuzzified output provides an interpretable crop condition decision with confidence, which is transmitted to a remote monitoring platform along with annotated visual evidence

2.7.1 Mathematical Formulation of the YOLOv7–Fuzzy Reasoning Framework

Let an input RGB image captured at time t be denoted as

$$I_t \in \mathbb{R}^{H \times W \times 3}, \quad \text{(Equation.1)}$$

where H and W represent the image height and width, respectively. The image I_t is processed by the YOLOv7 detector, which outputs a set of object detections defined as

$$D_t = \{(b_i, c_i, s_i)\}_{i=1}^{N_t}, \quad \text{(Equation.2)}$$

where b_i denotes the bounding box coordinates of the i-th detected object, $c_i \in \mathcal{C}$ is the predicted class label, $s_i \in [0,1]$ is the associated confidence score, and N_t represents the total number of detections at time t. In this study, the class set is defined as

$$\mathcal{C} = \{\text{healthy leaf,wilt leaf,flower,fruit}\}. \quad \text{(Equation.3)}$$

To obtain meaningful agronomic indicators, detections are aggregated over each observation period to compute class-wise object counts:

$$x_j = \sum_{i=1}^{N_t} \mathbb{1}\,(c_i = j), j \in \mathcal{C}, \tag{Equation.4}$$

where $\mathbb{1}(\cdot)$ denotes the indicator function. In addition to visual information, temporal growth context is incorporated through a cultivation-stage variable w, defined as

$$w = \lfloor \frac{t - t_0}{7} \rfloor + 1, \tag{Equation.5}$$

where t_0 represents the planting date and w corresponds to the number of weeks elapsed since cultivation began. Based on these components, a crisp agronomic feature vector is constructed as

$$\mathbf{X} = [H_{\text{leaf}}, W_{\text{leaf}}, F_{\text{flower}}, F_{\text{fruit}}, \text{Week}], \tag{Equation.6}$$

where H_{leaf} and W_{leaf} denote the total numbers of detected healthy and wilted leaves, F_{flower} and F_{fruit} represent the detected counts of flowers and fruits, respectively, and Week indicates the cultivation stage. This feature vector integrates visual perception with temporal growth information and serves as the crisp input to the fuzzy inference system.

Each element of $\mathbf{X}$ is fuzzified using predefined membership functions $\mu_k(\cdot)$, which map numerical values into interpretable linguistic terms such as Low, Medium, and High. A Mamdani-type fuzzy inference system is employed, consisting of a rule base

$$\mathcal{R} = \{R_1, R_2, \dots, R_M\}, \tag{Equation.7}$$

where each rule R_m takes the general form:

$$\text{IF } x_1 \text{ is } A_1^m \wedge \cdots \wedge \text{Week is } A_5^m \text{ THEN } y \text{ is } B^m. \tag{Equation.8}$$

Here, m denotes the index of the fuzzy rule within the rule base, and M represents the total number of rules. The symbols A_k^m correspond to fuzzy sets associated with the k-th input variable in the m-th rule, representing linguistic terms such as Low, Medium, or High. The term B^m denotes the fuzzy output set of the m-th rule, corresponding to a crop condition category. This formulation allows each rule to encode expert agronomic knowledge linking specific growth indicators and temporal stages to interpretable decision outcomes. The inference process follows the min–max composition principle, enabling the aggregation of multiple rules to model uncertainty and nonlinear interactions among agronomic factors. The aggregated fuzzy output is converted into a crisp decision using the centroid defuzzification method:

$$y^* = \frac{\int y\, \mu_Y(y)\, dy}{\int \mu_Y(y)\, dy}, \qquad \text{(Equation.9)}$$

where y^*represents the final crop condition index and $\mu_Y(y)$ denotes the aggregated output membership function. The resulting value is mapped to actionable agronomic decision categories, including Normal Condition, Check Wilt Leaf, Check Flower, Check Fruit, and Abnormal Condition, along with an associated confidence score.

Through this formulation, the proposed YOLOv7–fuzzy reasoning framework effectively transforms noisy and imbalanced object-level detections into stable, interpretable, and growth-aware crop condition assessments. By explicitly integrating temporal context and expert agronomic knowledge, the system bridges data-driven perception and decision-level reasoning, enhancing robustness and practical applicability in real greenhouse environments.

2.7.2 Transparency of the Fuzzy Reasoning Mechanism

To enhance interpretability and reproducibility, the structure and formulation of the fuzzy reasoning mechanism are explicitly described. The fuzzy inference system operates on an agronomic feature vector as depicted in Equation 6, where the elements represent aggregated counts of healthy leaves, wilted leaves, flowers, fruits, and the cultivation week, respectively. Each input variable is mapped to linguistic terms using triangular membership functions, enabling gradual transitions between plant growth conditions rather than rigid threshold-based decisions.

Membership functions were designed based on empirical observations across multiple cultivation seasons and expert agronomic knowledge. For instance, the healthy leaf variable is fuzzified into Low, Medium, and High, corresponding to sparse foliage typical of early or stressed growth, balanced vegetative development, and dense canopy formation associated with vigorous plant health. Similarly, the temporal variable Week is fuzzified into first four weeks, second four weeks, and last four weeks, representing early vegetative establishment, flowering transition, and fruit maturation stages, respectively. Allowing membership functions to extend beyond the physical input range ensures smooth boundary behavior; during inference, all crisp inputs are clipped to their valid domains prior to fuzzification. The full specification of input and output membership functions is summarized in Table 3.

Table 3 Membership functions used in the fuzzy inference system (triangular parameters [a, b, c]).

Variable	Universe	Linguistic terms and parameters [a, b, c]
Health_leaf	0–170.01	Low [-70.83, 0, 60]; Medium [14.17, 85, 155]; High [99.47, 170.3, 241.1]
Wilt_leaf	0–160.01	Small [-66.39, 0, 40]; Middle [14, 80, 140]; Larger [80, 162, 229]
Flower	0–150.01	Few [-62.81, 0, 30]; Moderate [15, 75, 130]; Too_much [87.51, 150, 212.4]
Fruit	0–80.01	Little [-33.33, 0, 20]; Somehow [15, 40, 70]; Many [50, 80, 113.3]
Week	0–12.01	First_four_weeks [-5, 0, 6]; Second_four_weeks [4, 7, 10]; Last_four_weeks [8, 12, 17]
Rock_melon (output)	0–150.01	Normal [-37.5, 0, 37.5]; Check_wilt_leaf [10, 37.5, 75]; Check_flower [37.5, 75, 112.5]; Check_fruit [75, 112.5, 150]; Abnormal [112.5, 150, 187.5]

The fuzzy rule base was constructed to encode agronomic knowledge governing cantaloupe growth progression across temporal stages. The system employs 243 expert-defined rules, derived from the full combinatorial set of 3 linguistic terms for each of the 5 input variables (i.e., $3^5 = 243$) (73,74). This exhaustive coverage ensures the system can logically evaluate all plausible growth scenarios. Rules jointly consider plant health indicators (healthy and wilted leaf abundance), reproductive development (flower and fruit counts), and cultivation stage to derive condition-level assessments. Temporal segmentation allows identical visual observations to be interpreted differently depending on biological context, reflecting real-world agronomic reasoning.

For example, low healthy leaf counts combined with few flowers and fruits during early cultivation are interpreted as normal establishment behavior, whereas the same pattern during mid or late stages indicates abnormal development due to insufficient vegetative or reproductive progression. Excessive flowering during late stages without proportional fruit development triggers a Check Flower condition, signalling potential stress or resource imbalance. High fruit counts during early stages prompt a Check Fruit decision to verify premature fruiting, while similar observations during later stages are considered normal maturation behavior. Representative rules illustrating this reasoning include:

I. R_1: IF healthy leaf count is low AND wilted leaf count is small AND flowers are few AND fruits are few during early cultivation, THEN crop condition is *Normal*.

II. R_2: IF healthy leaf count is low AND flowers remain few during mid or late cultivation, THEN crop condition is *Abnormal*.

III. R_3: IF flowers are excessive during late cultivation, THEN crop condition is *Check Flower*.

IV. R_4: IF fruit count is high during early cultivation, THEN crop condition is *Check Fruit*.

V. R_5: IF fruit count is high AND wilted leaves remain low during late cultivation, THEN crop condition is *Normal*.

Inference is performed using a Mamdani-type fuzzy reasoning scheme with min–max composition, and the aggregated output is defuzzified using the centroid method to produce a continuous crop condition index. The final agronomic decision is obtained by mapping the defuzzified value to the output linguistic class with the highest membership degree. The associated confidence score reflects the strength of activation of the selected output membership function rather than a probabilistic estimate, enabling uncertainty-aware interpretation of noisy or ambiguous visual detections. This transparent formulation allows the fuzzy reasoning module to stabilize frame-level detection variability, absorb class imbalance effects, and translate vision-based outputs into consistent and interpretable agronomic decisions suitable for practical deployment. The complete fuzzy inference system comprises 243 expert-defined rules, providing comprehensive combinatorial coverage of the input space.

2.7.3 YOLOV7 model Details

Fig. 4 (a) show the YOLOv7 model adopted in this study which serves as the core visual perception module for cantaloupe growth analysis, with its detection outputs subsequently processed by a fuzzy reasoning layer for decision-level inference (44,73,74). YOLOv7 was selected due to its strong balance between detection accuracy, inference efficiency, and architectural stability under challenging agricultural conditions.

During the input preprocessing stage, mosaic and hybrid data augmentation strategies are applied to enhance robustness against illumination variation and occlusion, while images are resized to a fixed resolution of 640×640×3 (19,43). The backbone network is composed of convolution–batch normalization–SiLU (CBS) blocks, Efficient Layer Aggregation Network (E-ELAN) modules for improved gradient flow and feature diversity, and max-pooling (MP) layers for multi-scale feature abstraction (51–53,75).

The neck architecture integrates a Feature Pyramid Network (FPN) with a Path Aggregation Network (PAN) to enable effective multi-scale feature fusion, which is further enhanced using Spatial Pyramid Pooling and Convolutional Spatial Pyramid Pooling (SPPCSPC) blocks to enlarge the receptive field without increasing computational cost (1,13,42,47). The detection head employs RepConv structures inspired by RepVGG, allowing complex multi-branch representations during training to be re-parameterized into simple convolutional layers at inference time, thereby improving efficiency while preserving accuracy (51–53,75,76).

The final output of the YOLOv7 detector consists of bounding box coordinates, class labels, and confidence scores for healthy leaves, wilted leaves, flowers, and fruits. These outputs form the input to the fuzzy reasoning module, which performs temporal aggregation and uncertainty-aware decision making for crop condition assessment as depicted in Fig. 4(b).

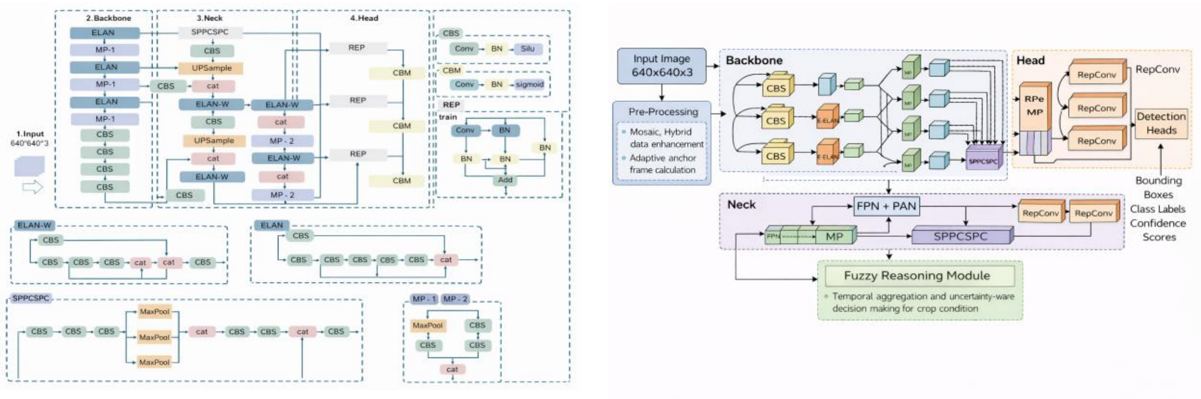

Fig. 4 Architecture of the proposed YOLOv7-based cantaloupe growth analysis framework: (a) internal structure of the YOLOv7 detector, including backbone, neck, and head components (52,53,75); (b) integration of YOLOv7 detection outputs with the fuzzy reasoning module for temporal and uncertainty-aware crop condition assessment

2.8 Experimental Environment and Training Configuration

In this study (19,47,55), all experiments were conducted on a desktop workstation equipped with an 11th Generation Intel® Core™ i7-11700K processor (3.60 GHz) and an NVIDIA GeForce RTX 3060 GPU with 12 GB VRAM, providing sufficient computational resources for stable training and convergence of deep convolutional models. The software environment consisted of Python 3.10.19, PyTorch 1.13.1 with CUDA acceleration, Torchvision 0.14.1, OpenCV-Python 4.11.0.86, and Scikit-Fuzzy 0.5.0. This configuration ensured efficient GPU-accelerated training and seamless integration between deep learning–based perception and fuzzy logic–based reasoning modules.

Input images were resized to 640 × 640 pixels prior to training. The YOLOv7 detector was initialized with weights pre-trained on the MS COCO dataset to leverage transfer learning and accelerate convergence. Model optimization was performed using stochastic gradient descent (SGD) with an initial learning rate of 0.01, momentum of 0.937, and weight decay of 0.0005. Training was carried out for up to 100 epochs with a batch size of 30, allowing full end-to-end optimization of both the backbone and detection heads. Single-scale training was adopted to maintain consistent receptive field learning, while rectangular training was disabled to avoid aspect-ratio bias that could distort plant organ geometry.

The loss function was configured using a balanced weighting strategy to accommodate heterogeneous plant structures and address class imbalance within the dataset. Specifically, the bounding box regression loss weight was set to 0.05, the objectness loss weight to 0.7, and the classification loss weight to 0.3. An Intersection-over-Union (IoU) threshold of 0.2 was used for positive sample assignment, with an anchor matching threshold fixed at 4.0. These settings were selected to promote stable localization and classification under challenging greenhouse conditions, including partial occlusion, overlapping leaves, and visually similar plant organs.

To enhance generalization and robustness against environmental variability, several data augmentation strategies were employed during training. Mosaic augmentation was enabled to increase contextual diversity and encourage multi-scale feature learning, while MixUp augmentation was applied with a ratio of 0.15 to reduce overfitting and smooth class boundaries. Color-space perturbations were introduced using HSV augmentation (hue = 0.015, saturation = 0.7, value = 0.4) to simulate illumination changes, and horizontal flipping was applied with a probability of 0.5 to improve viewpoint invariance. Copy–paste augmentation was intentionally disabled to prevent the creation of unrealistic plant structures that could negatively affect agronomic interpretability.

Following object detection, a Mamdani-type fuzzy inference system was applied during the inference stage to integrate aggregated YOLOv7 outputs with temporal growth information. The fuzzy module was implemented using the Scikit-Fuzzy library, with NumPy supporting numerical operations and Matplotlib used for visualization. This modular separation between deep learning–based visual perception and fuzzy rule-based reasoning ensures stable training, interpretability, and decision-level robustness, which are essential for reliable deployment in precision agriculture applications.

2.9 Accuracy Evaluation Metrics

The assessment of detection performance included precision (P) equation 10, recall (R) equation 11, F1-Score (F1) equation 12, average precision (AP) equation 13, and mAP equation 14 (11,23,45,50).

$$Precission(Pr) = \frac{TP}{TP + FP} \qquad \text{(Equation.10)}$$

$$Recall(Rc) = \frac{TP}{TP + FN} \qquad \text{(Equation. 11)}$$

$$F1 - score(F1) = 2 \times \frac{Precision \times Recal}{Precision + Recall} \qquad \text{(Equation. 12)}$$

$$Ap = \int_{0}^{1} Pr(Rc)\, dRc \qquad \text{(Equation. 13)}$$

$$mAP = \frac{1}{n} \sum_{k=1}^{k=n} AP_k \qquad \text{(Equation.14)}$$

In this case, Pr represents the accuracy of correct detections, Rc represents the percentage of cantaloupe classes accurately identified by the network. F1 represents overall performance considering both Pr and Rc, while mAP corresponds to the average value of each type of AP. True positives, false positives, and false negatives are established based on confidence levels and IoU thresholds. TP indicates a cantaloupe class correctly identified as a flower, fruit, healthy leaf or wilted leaf; FP denotes background erroneously recognized as one of these categories; FN pertains to an undetected flower, fruit, healthy leaf or wilted leaf. Precision and recall are calculated from TP, FP, and FN, and F1-score is derived from Pr and Rc.

3 Results

This section presents and analyzes the experimental results obtained from training and evaluating multiple YOLO-based detectors, followed by the integration of fuzzy reasoning for decision-level interpretation. The discussion emphasizes comparative performance, class-level behavior, and the practical implications of combining deep learning with fuzzy logic for cantaloupe growth-stage assessment.

3.1 Overall Detection Performance

Table 4 summarizes the quantitative performance of YOLOv5s, YOLOv7, YOLOv8n, and YOLOv8s on the proposed dataset. Among the evaluated models, YOLOv7 achieved the highest overall detection accuracy, with a precision of 0.721, recall of 0.758, and mAP@0.5 of 0.771. Although YOLOv5s demonstrated slightly higher precision, its substantially lower recall indicates a tendency to miss objects, which is undesirable for agronomic monitoring where false negatives may lead to delayed intervention. YOLOv8 variants showed competitive performance but exhibited reduced robustness under the dataset's real greenhouse conditions, likely due to sensitivity to occlusion, variable lighting, and dense foliage. These results indicate that YOLOv7 offers the most balanced trade-off between detection accuracy and consistency, making it a suitable backbone for downstream agronomic reasoning.

Table 4 . Presents the quantitative comparison of YOLOv5s, YOLOv7, YOLOv8n, and YOLOv8s under identical training and evaluation settings.

Model	Precision	Recall	mAP@0.5	mAP@0.5:0.95
YOLOv5s	0.752	0.675	0.722	0.462
YOLOv7	0.721	0.758	0.771	0.523
YOLOv8n	0.716	0.658	0.704	0.460
YOLOv8s	0.706	0.719	0.732	0.489

3.1.1 Per-Class Detection Performance and Class Imbalance Effects

The per-class performance comparison in Table 5 reveals distinct and systematic behavior across detection models when applied to an imbalanced cantaloupe dataset. Although all models achieve competitive performance, notable trade-offs between precision and recall are observed across plant organs, highlighting the inherent uncertainty of vision-based perception in dense agricultural environments. For instance, healthy leaf detection shows higher recall in YOLOv8s (0.815) but at the cost of reduced precision (0.545), indicating increased false positives under foliage overlap and background clutter. In contrast, YOLOv7 achieves a more balanced trade-off between precision (0.627) and recall (0.701), resulting in a stable mAP@0.5 of 0.671.

A similar trend is evident in wilted leaf detection, where YOLOv7 attains the highest recall (0.707) and mAP@0.5 (0.706), despite only moderate precision. This suggests that YOLOv7 effectively captures subtle visual cues associated with early stress symptoms, even when class distributions are skewed. Flower detection further illustrates the limitations of single-stage detectors: while precision remains consistently high across models, recall varies significantly, with YOLOv7 demonstrating a substantial improvement (0.705) compared to YOLOv8n (0.503). This variability reflects the sensitivity of flower appearance to occlusion, scale variation, and growth-stage transitions.

Fruit detection exhibits the highest overall accuracy for all models due to its distinctive morphology and color contrast; however, YOLOv7 again achieves the highest recall (0.919) and mAP@0.5 (0.930), reinforcing its robustness under real greenhouse conditions. Importantly, these results indicate that performance gains are not uniformly distributed across classes and are strongly influenced by class imbalance, visual ambiguity, and temporal growth dynamics (see Section 2.6). While deep detectors successfully learn discriminative features, their outputs remain probabilistic and occasionally conflicting across growth indicators. These class-specific performance trade-offs, inherent to data-driven detectors operating on imbalanced data, underscore the necessity for a subsequent reasoning layer. The proposed fuzzy inference system addresses this by explicitly modelling uncertainty and agronomic context to generate stable condition assessments from these variable detection outputs.

Table 5. Per-class detection performance comparison of YOLOv5s, YOLOv8n, YOLOv8s, and YOLOv7 on the cantaloupe growth dataset.

Class	Metric	YOLOv5s	YOLOv8n	YOLOv8s	YOLOv7
	Precision	0.650	0.612	0.545	0.627
Healthy leaf	Recall	0.673	0.736	0.815	0.701
	mAP@0.5	0.668	0.721	0.711	0.671
	Precision	0.683	0.635	0.619	0.643
Wilt leaf	Recall	0.593	0.642	0.696	0.707
	mAP@0.5	0.645	0.680	0.691	0.706
	Precision	0.815	0.776	0.812	0.820
Flower	Recall	0.613	0.503	0.560	0.705
	mAP@0.5	0.701	0.610	0.677	0.779
	Precision	0.859	0.840	0.850	0.794
Fruit	Recall	0.820	0.751	0.804	0.919
	mAP@0.5	0.875	0.804	0.849	0.930

The observed class-dependent performance variations do not indicate detector failure but rather reflect the intrinsic uncertainty of vision-based perception in dense agricultural environments. Minority classes such as flowers and fruits exhibit higher sensitivity to occlusion, scale variation, and growth-stage transitions. These results reinforce the limitation of relying solely on per-frame detection metrics for agronomic decision-making and highlight the necessity of a higher-level reasoning mechanism capable of integrating multi-class cues and temporal context.

3.2 Temporal Growth Behavior and Detection Stability

Beyond static performance metrics, the temporal analysis of detections across cultivation weeks provides critical insight into model behavior under realistic agronomic conditions. YOLOv7 demonstrated consistent detection trends that closely align with expected biological growth patterns, including gradual increases in flower and fruit counts during mid to late cultivation stages. In contrast, other evaluated models exhibited higher variability across weeks, indicating increased sensitivity to environmental noise, occlusion, and viewpoint changes. Such temporal stability is essential for growth-stage analysis, as agronomic decisions rely not on isolated detections but on coherent trends observed over time.

Fig. 5 presents a qualitative comparison of detection performance across four representative single-stage detectors—YOLOv5s, YOLOv8n, YOLOv8s, and YOLOv7—under both high-resolution and low-resolution imaging conditions within a real greenhouse environment. In high-resolution scenes, all models are capable of identifying major plant organs; however, notable differences emerge in detection stability, confidence consistency, and class separation. Lightweight architectures such as YOLOv5s and YOLOv8n tend to produce dense yet fragmented detections, particularly for wilted leaves and fruits, with frequent overlapping bounding boxes and fluctuating confidence scores. This behavior reflects sensitivity to background clutter and inter-leaf occlusion, resulting in over-detection and increased instance-level ambiguity.

Under low-resolution conditions-more representative of practical deployment scenarios involving camera distance, bandwidth limitations, and illumination degradation these differences become more pronounced. While YOLOv8s achieves strong recall under high-resolution settings, it exhibits confidence collapse and missed detections as spatial detail diminishes, occasionally failing to detect target objects altogether. In contrast, YOLOv7 maintains comparatively stable detections across both resolution regimes, preserving semantic coherence among healthy leaves, wilted leaves, flowers, and fruits despite partial occlusion and reduced image fidelity. This robustness can be attributed to YOLOv7's architectural balance between network depth, feature aggregation, and receptive field expansion, enabling effective multi-scale representation without excessive noise amplification.

Importantly, the qualitative evidence in Fig. 5 demonstrates that high numerical detection accuracy alone does not guarantee reliable agronomic interpretation under real-world visual uncertainty. Models that generate dense or unstable detections tend to propagate noise into downstream decision processes, undermining consistent growth-stage assessment. In contrast, the structured and temporally stable outputs produced by YOLOv7 provide a more reliable foundation for decision-level reasoning. These characteristics make YOLOv7 particularly suitable for integration with fuzzy inference, where robust agronomic decisions benefit from consistent yet flexible input signals rather than maximal instance counts. This observation justifies the selection of YOLOv7 as the backbone detector in the proposed YOLOv7–Fuzzy framework, prioritizing robustness and interpretability over raw detection density. These factors limit the direct interpretability of frame-level predictions and highlight the need for a higher-level reasoning mechanism capable of transforming raw detections into robust and agronomically meaningful decisions.

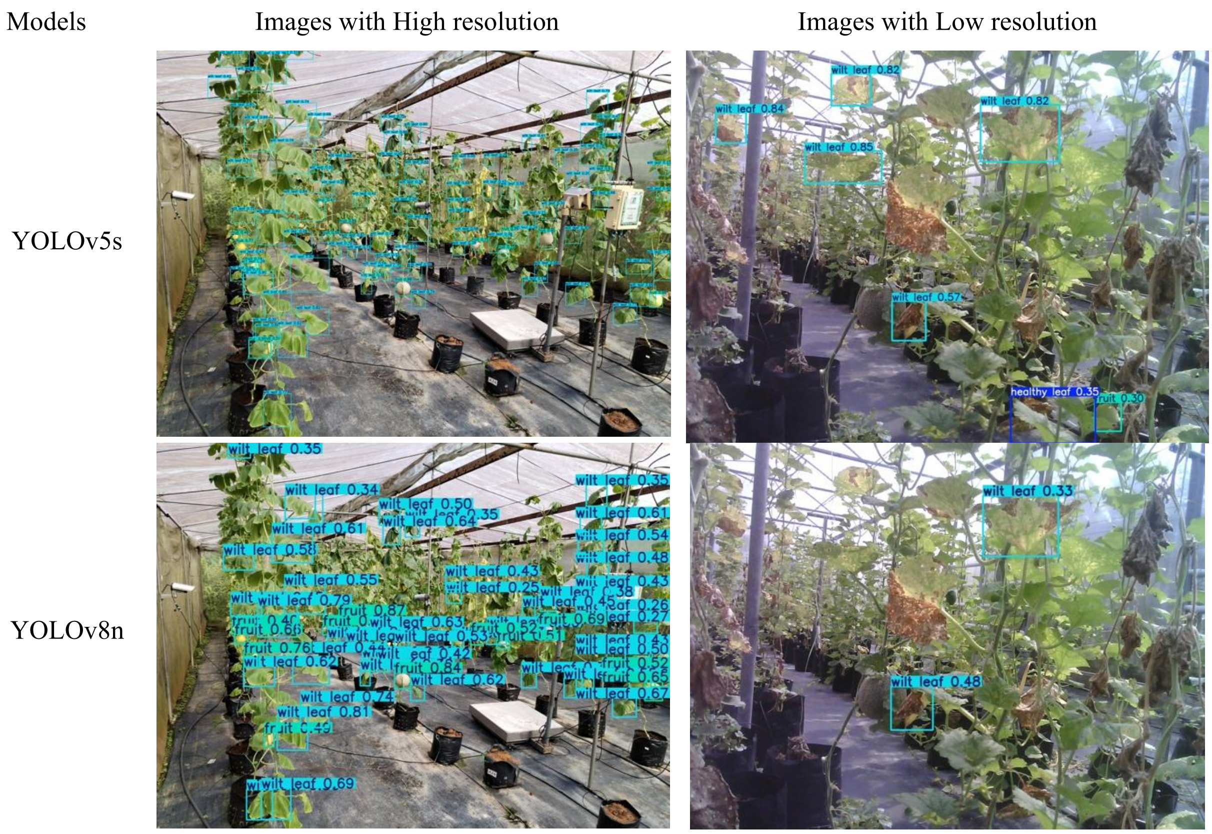

YOLOv8s

YOLOv7

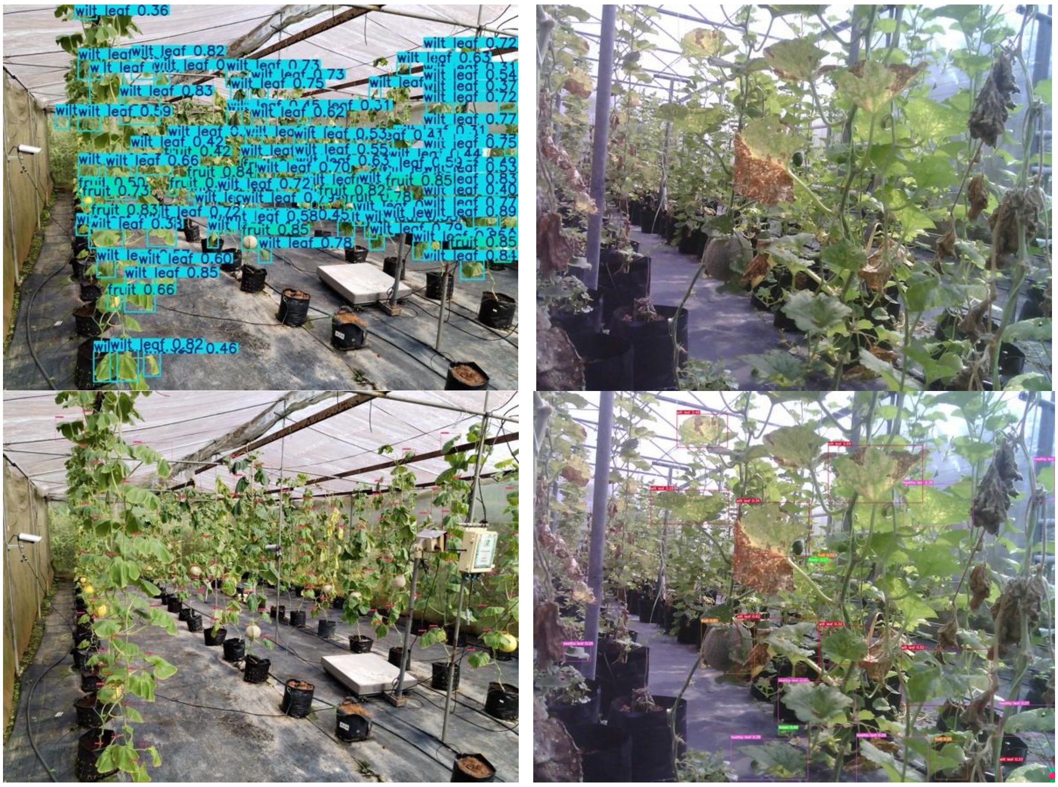

Fig. 5 Qualitative comparison of detection performance across YOLOv5s, YOLOv8n, YOLOv8s, and YOLOv7 under high- and low-resolution greenhouse conditions. YOLOv7 exhibits superior detection stability and semantic consistency across resolution variations, motivating its selection as the backbone for fuzzy reasoning integration

3.2.1 Derived Growth Patterns and Fuzzy Knowledge Base Formulation

To derive a robust and transferable fuzzy knowledge base, longitudinal detection outputs from eleven cultivation cycles across three geographically distinct greenhouse sites were analyzed. These cycles span varying environmental conditions, camera configurations, and management practices, thereby capturing realistic variability in cantaloupe growth. Rather than relying on single-season observations, this multi-cycle analysis enables the extraction of generalized phenological patterns representative of standard greenhouse cultivation.

Fig. 6 presents the class-specific temporal detection trends aggregated per cultivation cycle. Healthy leaf abundance Fig. 6 (a) exhibits rapid early-stage growth, peaking between weeks 3 and 4, followed by a gradual decline as plant resources are redirected toward reproductive development. In contrast, wilted leaves Fig. 6 (b) remain minimal during early growth stages and increase markedly after week 8. This behavior is consistent with controlled stress induction commonly applied during fruit maturation to enhance sugar accumulation (77). Flowering dynamics Fig. 6 (c) show a narrow and well-defined window, with a sharp peak at week 4 and near-complete senescence by week 9. Fruit development Fig. 6 (d) initiates shortly after flowering, increases steadily to a maximum around week 9, and subsequently declines as harvesting begins. While these patterns are biologically consistent, noticeable inter-season variability underscores the need for a generalized temporal reference rather than season-specific thresholds.

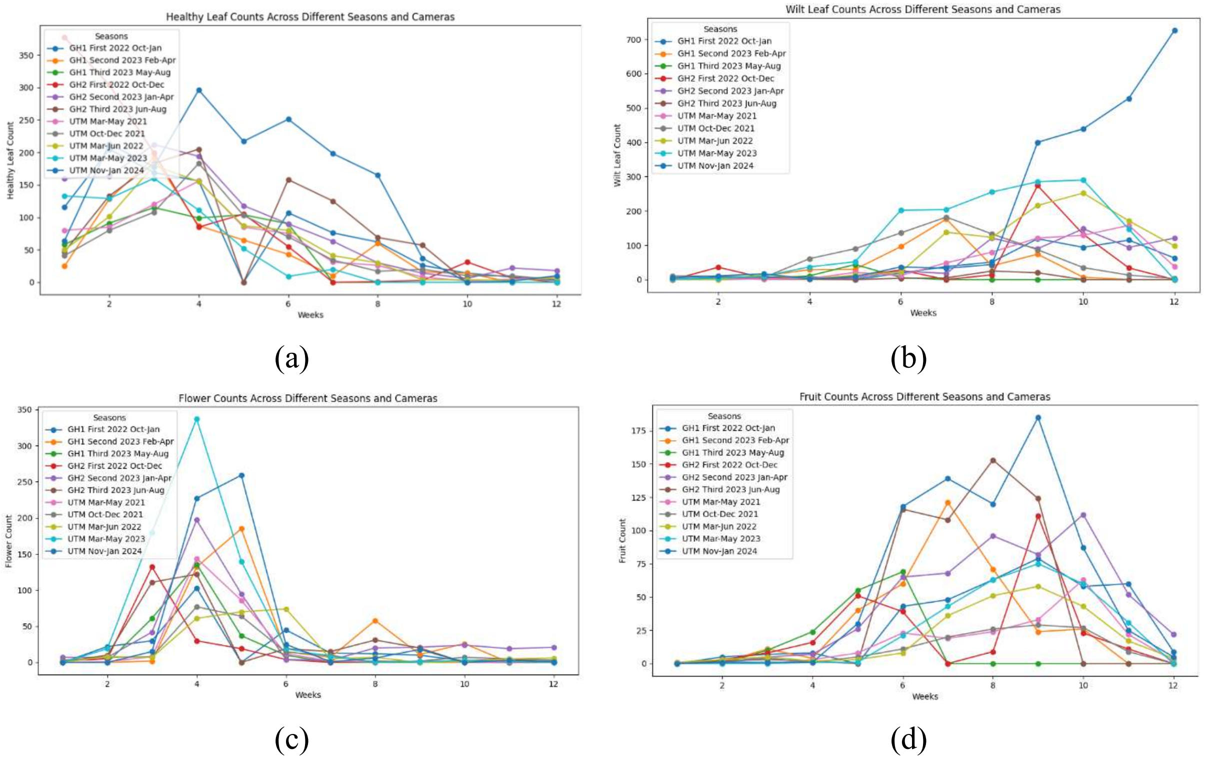

Fig. 6 Class-specific temporal detection trends across multiple cultivation cycles for (a) healthy leaves, (b) wilted leaves, (c) flowers, and (d) fruits, illustrating inter-season variability in cantaloupe growth behavior

To eliminate season-dependent fluctuations and extract a canonical growth trajectory, a per-week average across all cultivation cycles was computed using the arithmetic mean represented by Equation.15:

$$A = \frac{1}{n}\sum_{i=1}^{n} a_i, \qquad \text{(Equation.15)}$$

where n denotes the number of cultivation cycles and a_i represents the class-specific detection count for cycle i. The resulting averaged trends are shown in Fig. 7. This season-invariant representation smooths episodic anomalies caused by environmental disturbances, occlusion effects, and transient detection noise, revealing consistent biological relationships between agronomic indicators.

The averaged curves define critical temporal transitions that are agronomically meaningful. Notably, fruit counts consistently surpass flower counts after approximately week 6, marking successful fruit set, while wilted leaf abundance exceeds healthy leaf counts after week 8 under standard stress-for-quality cultivation protocols. These transitions are not enforced as rigid thresholds but serve as soft temporal benchmarks against which real-time observations are evaluated.

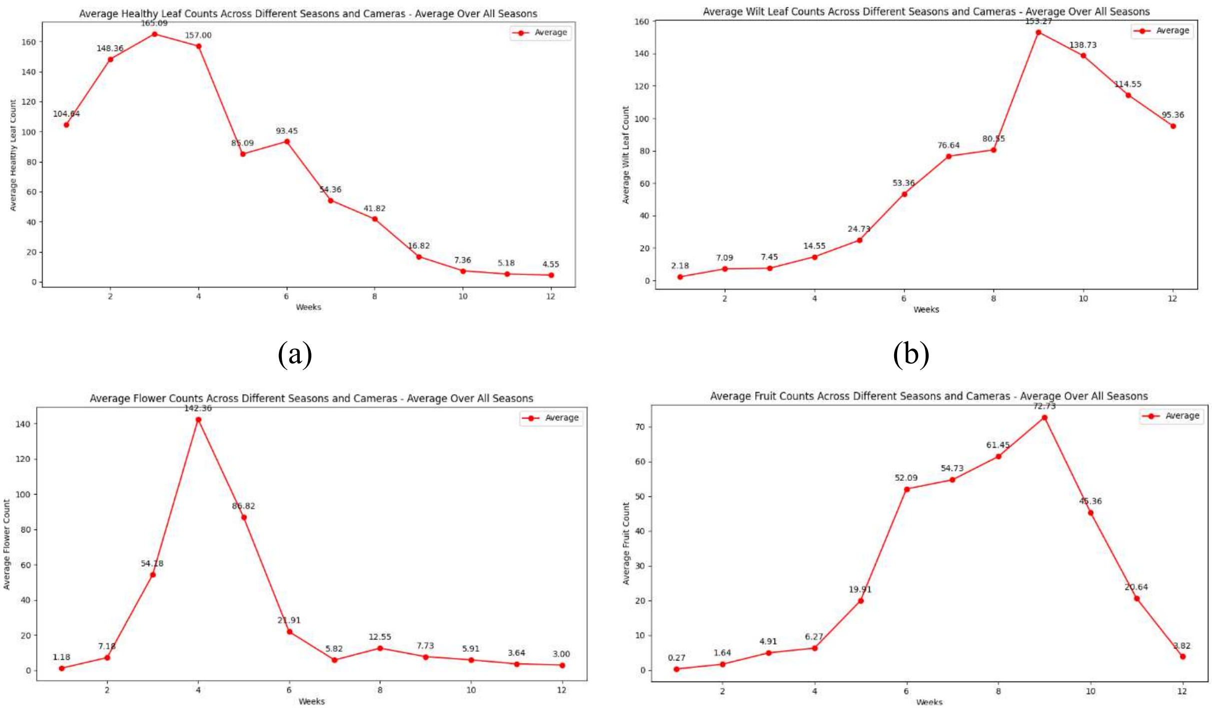

(a) (b)

(c) (d)

Fig. 7 Per-week averaged temporal growth trends computed across all cultivation cycles for (a) healthy leaves, (b) wilted leaves, (c) flowers, and (d) fruits, revealing a season-invariant canonical growth trajectory

Based on these averaged patterns, an integrated temporal growth signature was formalized, as illustrated in **Fig. 8.** This signature represents the expected progression of healthy leaves, wilted leaves, flowers, and fruits throughout the twelve-week cultivation cycle. Importantly, this growth signature does not prescribe an exact numeric trajectory but instead defines relative temporal relationships among plant organs, which are more resilient to detection noise and class imbalance.

This integrated growth signature forms the foundation of the Mamdani-type fuzzy inference system. Each fuzzy rule compares aggregated detection outputs against these canonical temporal relationships rather than absolute counts, enabling the system to distinguish between normal developmental progression and anomalous conditions requiring intervention. By grounding the fuzzy rule base in empirically derived, season-invariant trends, the proposed framework ensures that decision-level reasoning remains biologically meaningful, interpretable, and robust across varying greenhouse conditions.

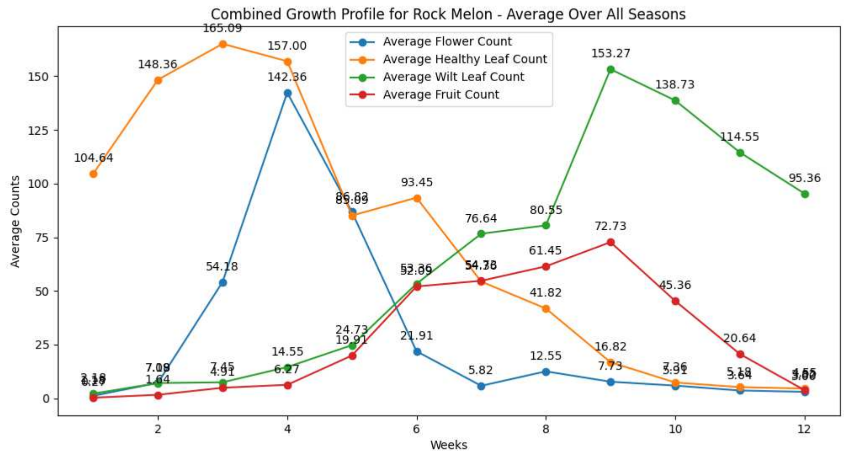

Fig. 8 Integrated canonical growth signature of cantaloupe derived from averaged detection trends, used as the agronomic reference for fuzzy rule formulation and decision-level reasoning

3.3 Impact of Fuzzy Reasoning on Decision-Level Interpretation

While YOLOv7 provides reliable object-level detections, raw detection counts alone are insufficient to support actionable agronomic decisions due to uncertainty, class imbalance, and temporal fluctuations. The integration of fuzzy reasoning addresses these limitations by transforming detection outputs into a structured agronomic assessment. By aggregating detected healthy leaves, wilted leaves, flowers, fruits, and cultivation week into a unified feature vector, the fuzzy system produces interpretable crop condition states with associated confidence levels. This decision-level abstraction reduces sensitivity to sporadic detection errors and enables human-like reasoning that aligns with expert agronomic knowledge.

3.4 Ablation Study: Impact of Fuzzy Reasoning Integration

To evaluate the contribution of the fuzzy reasoning module beyond object detection, an ablation study was conducted by comparing two system configurations: (i) the baseline YOLOv7 detector and (ii) the proposed YOLOv7–fuzzy reasoning framework. The baseline system produces frame-level object detections and standard performance metrics, whereas the proposed framework extends these outputs by aggregating detections temporally and applying expert-defined fuzzy rules to infer high-level crop condition states.

The ablation analysis reveals that, although YOLOv7 alone achieves strong detection performance, it lacks the ability to explicitly encode temporal dependencies and semantic relationships among agronomic indicators. As a result, raw detection counts must be manually interpreted, which is impractical under real greenhouse conditions where detection noise, class imbalance, and seasonal variability are unavoidable. In contrast, the fuzzy-enhanced framework introduces a decision-level reasoning layer that transforms fluctuating object counts into stable, agronomically meaningful condition assessments.

Importantly, the fuzzy reasoning module operates exclusively as a post-detection inference layer and does not alter the training or optimization of YOLOv7. Consequently, detection accuracy is preserved while interpretability and decision robustness are significantly improved. By embedding agronomic knowledge and temporal growth context, the fuzzy layer enables early identification of anomalous growth behavior—such as delayed flowering, excessive wilting, or premature fruiting—even when individual detections vary across frames.

Table 6. Qualitative Ablation Comparison Between YOLOv7 and YOLOv7–Fuzzy Framework

Configuration	Output Level	Temporal Growth Awareness	Decision Consistency Across Weeks	Interpretability for Agronomic Decision-Making
YOLOv7 only	Object-level detections (leaf, flower, fruit counts)	Absent	Sensitive to frame-to-frame variation	Limited requires manual interpretation of raw counts
YOLOv7 + Fuzzy Logic	Semantic crop-condition state with confidence score	Integrated via growth-stage rules	Improved — outputs stabilized by temporal and agronomic constraints	High provides biologically meaningful states (e.g., *Normal*, *Check Flower*, *Abnormal*)

This ablation study confirms that the primary contribution of fuzzy reasoning lies not in marginal gains in detection metrics, but in elevating the system from a conventional object detector to a practical decision-support tool. As summarized in Table 6

Configuration	Output Level	Temporal Growth Awareness	Decision Consistency Across Weeks	Interpretability for Agronomic Decision-Making
YOLOv7 only	Object-level detections (leaf, flower, fruit counts)	Absent	Sensitive to frame-to-frame variation	Limited requires manual interpretation of raw counts
YOLOv7 + Fuzzy Logic	Semantic crop-condition state with confidence score	Integrated via growth-stage rules	Improved — outputs stabilized by temporal and agronomic constraints	High provides biologically meaningful states (e.g., *Normal*, *Check Flower*, *Abnormal*)

, the baseline YOLOv7 configuration produces only raw object detections, whereas the proposed YOLOv7–fuzzy framework outputs semantically meaningful crop condition states with associated confidence levels. The qualitative impact of this decision-level abstraction is further illustrated in Fig. 9, which demonstrates how temporally aggregated detections are transformed into stable agronomic recommendations. Such abstraction is essential for precision agriculture applications, where actionable insights and confidence-aware recommendations are more valuable than raw detection density.

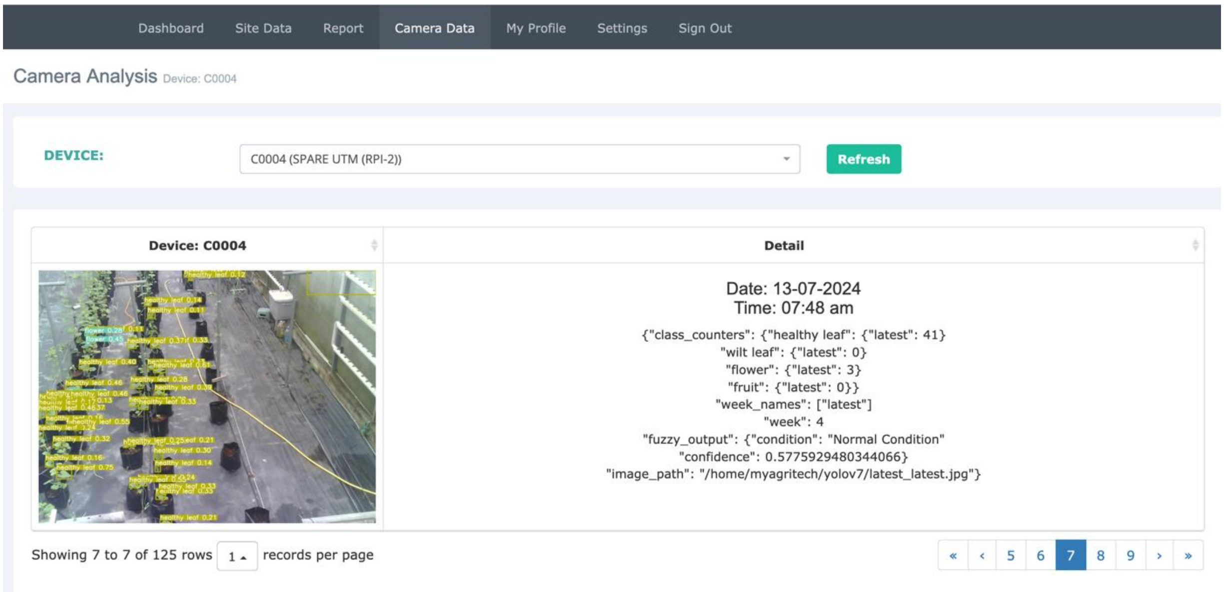

Fig. 9 Decision-level crop condition assessment produced by the proposed YOLOv7–fuzzy framework, illustrating the transformation of raw object detections into semantic agronomic states with associated confidence scores

3.4.1 Real-World Validation and Decision-Triggered Alerts

The practical efficacy of the proposed YOLOv7-Fuzzy framework was validated through real-time deployment on an NVIDIA Jetson Nano edge device (Jetson Nano B01 Beginner Kit, CK-JN-BG-V2) at multiple active farms, including Jengka GH1 (Pahang) and Putrajaya1 & 2 (see deployment setup, Fig. 10). The system processed images streamed from fixed cameras (C0019–C0024 at Jengka GH1) via the MyAgriTECH cloud server, performing on-device detection, weekly aggregation, and fuzzy inference. This deployment generated actionable, context-aware alerts that demonstrated the system's capacity for autonomous agronomic assessment.

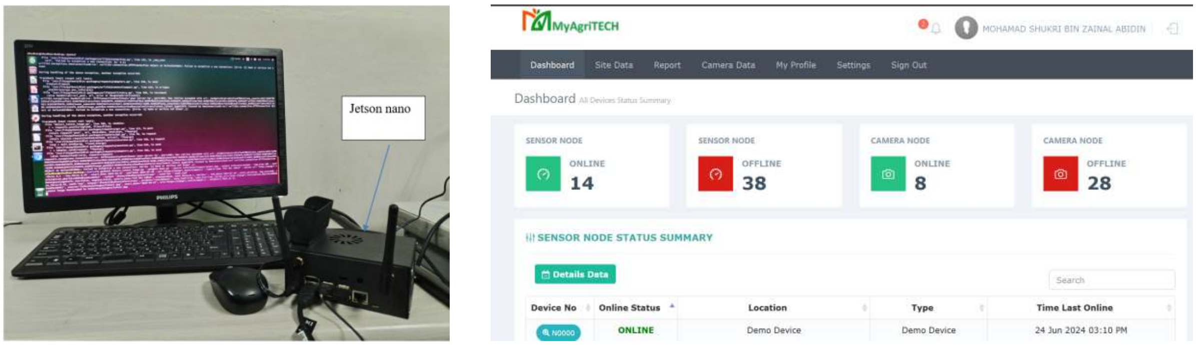

(a) (b)

Fig. 10 Real-world deployment architecture of the proposed YOLOv7–fuzzy framework on an NVIDIA Jetson Nano edge device, illustrating (a) the on-site edge inference setup and (b) the integration with fixed greenhouse cameras and the MyAgriTECH cloud server for real-time image streaming, detection, temporal aggregation, and decision-triggered alert generation

The fuzzy reasoning layer successfully translated detection counts into semantically meaningful decisions. For instance, at Jengka GH1 in week 5 post-cultivation (detected May 31, 2024), the system output a "Check flower" condition with 53% confidence as illustrated in Fig. 11 (a). This alert was triggered because the fuzzy rule for week 5 expects a higher flower-to-fruit ratio to ensure adequate pollination potential; the observed reversal of this ratio signalled a suboptimal state requiring inspection.

(a) (b)

Fig. 11 Examples of fuzzy reasoning–based decision outputs generated during real-world deployment: (a) "Check Flower" condition detected at Jengka GH1 during week 5 post-cultivation, indicating insufficient flowering relative to expected growth-stage patterns, and (b) "Normal Condition" detected at Putrajaya1 during week 11, where observed detection counts aligned with canonical growth trends

Conversely, the system also identified deviations from the expected canonical growth trend, triggering "Abnormal" condition alerts. As shown in Fig. 12 (b) for the Pahang GH1 site, multiple detections in the later cultivation stage (week 10 onward) resulted in high-confidence abnormal alerts (57.76%–63.87%). These alerts were generated by a specific agronomic rule encoded in the fuzzy system: during late-stage maturation (weeks 9–12), a controlled stress protocol is applied where wilted leaf count should exceed healthy leaf count to promote fruit sweetness. The model's detection—where healthy leaves still outnumbered wilted ones violated this expected physiological signature, prompting an immediate alert for farmer investigation. In parallel, the system correctly identified "Normal" conditions (Fig. 12 a) when observed metrics aligned with expected ranges, as seen at Putrajaya1 in week 11 (59% confidence, Fig. 11 (b)).

This real-world validation confirms that the framework moves beyond passive monitoring to active decision support. By fusing temporal context with expert-derived fuzzy rules, the system interprets raw detections to produce stable, interpretable alerts (e.g., "Check flower," "Abnormal condition") with associated confidence levels. This provides farmers with targeted guidance, transforming image data into prescriptive insights for timely intervention and optimized crop management.

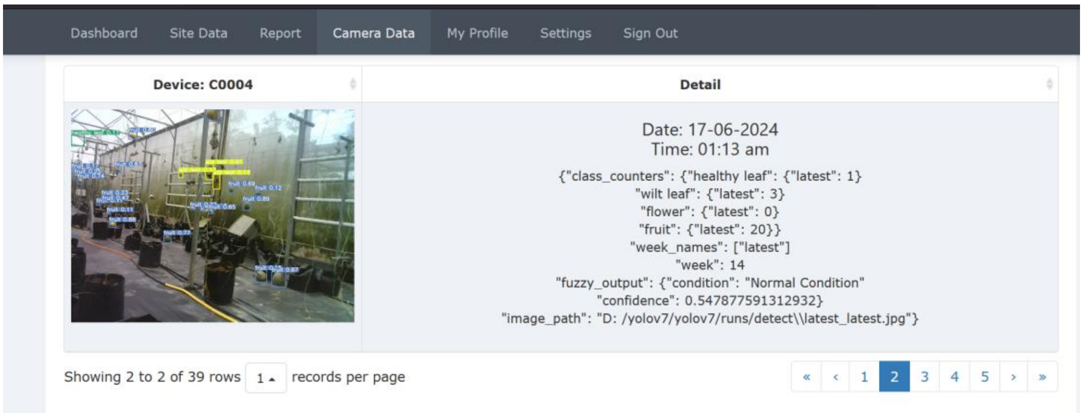

(a)

(b)

Fig. 12 Real-time detection and decision-triggered alerts generated by the YOLOv7–fuzzy framework under practical greenhouse conditions: (a) normal growth assessment at Putrajaya1, and (b)abnormal condition alerts at Jengka GH1 during late cultivation stages, where detected growth indicators deviated from the expected stress-induced physiological signature

4 Discussion

The transition from automated object detection to interpretable decision support remains a significant challenge in precision agriculture, particularly for high-value crops like cantaloupe where growth-stage assessment directly influences yield quality and resource allocation. This study proposes a hybrid YOLOv7–fuzzy reasoning framework to address this gap, demonstrating that integrating deep learning-based perception with knowledge-based reasoning can yield stable, actionable crop condition assessments under real greenhouse conditions. Below, we discuss the agronomic and methodological implications of our findings, contextualize them within existing research, and address the limitations and practical considerations of the proposed approach.

4.1 Bridging the gap between detection and decision in crop monitoring

Most vision-based systems in agriculture terminate at the object detection stage, providing farmers with counts or locations of plant organs but leaving the interpretation of those outputs to human expertise (14,15). While recent studies have improved detection accuracy under controlled conditions, few have explicitly addressed the temporal instability and class imbalance inherent in longitudinal crop imagery (18,27). Our framework introduces a fuzzy reasoning layer that operates on aggregated detection counts and cultivation time, transforming noisy per-frame predictions into semantically meaningful condition states (e.g., "Check Flower," "Abnormal Condition"). This aligns with the growing emphasis on explainable AI in agri-informatics, where model decisions must be interpretable and aligned with domain knowledge to facilitate trust and adoption (21,49). By encoding expert-derived phenological expectations into a fuzzy rule base, the system approximates agronomic reasoning patterns, thereby closing the loop between sensing and decision-making.

4.2 Robustness to real-world variability through temporal and contextual integration

Greenhouse environments introduce numerous challenges for vision systems, including illumination changes, occlusion, and varying plant densities. While data augmentation and model tuning can improve detector resilience, they do not eliminate frame-to-frame detection noise, especially for minority classes such as flowers. Our results show that YOLOv7 alone, despite achieving the highest mAP@0.5 among tested variants as shown in Table 4, still produces fluctuating counts across weeks. The fuzzy reasoning layer mitigates this by aggregating detections over time and evaluating them against canonical growth trends derived from multiple seasons. This temporal smoothing is agronomically justified, as crop development is a continuous process and decisions are based on trends rather than instantaneous observations. The system's ability to generate consistent alerts—such as flagging insufficient flowering in week 5 or detecting deviations from expected wilt patterns during maturation—demonstrates how contextual reasoning can compensate for perceptual uncertainty, a principle supported by earlier fuzzy logic applications in agricultural control and diagnosis (56,59,73,74).

4.3 Derivation and utility of canonical growth patterns

A key methodological contribution of this work is the use of multi-season, multi-site detection data to establish season-invariant growth signatures as depicted in figure Fig. 8. These patterns serve as a normative reference for fuzzy rule formulation, ensuring that the system's decisions are grounded in observed biological behavior rather than arbitrary thresholds. This approach differs from purely data-driven growth modeling, as it incorporates domain knowledge about expected transitions (e.g., flowering peaks precede fruiting) and management practices (e.g., controlled wilting for sweetness). The resulting fuzzy knowledge base is both interpretable and adaptable; rules can be modified or expanded as new agronomic insights emerge, without retraining the underlying detector. This flexibility is particularly valuable for crop varieties or cultivation environments that exhibit different phenological timelines, suggesting a pathway for transfer learning across contexts.

4.4 Limitations and future directions

While the proposed framework shows promise, several limitations should be acknowledged. First, the fuzzy rule base is currently static and based on expert knowledge from a specific cultivar (Glamour F1) and cultivation system (Malaysian greenhouses). Its performance in open fields, under different climatic conditions, or with other melon varieties requires further validation. Second, the system relies exclusively on visual cues; integrating non-visual data such as microclimate conditions, soil moisture, or nutrient levels could enhance diagnostic accuracy and enable more holistic crop assessment. Third, the confidence scores provided by the fuzzy system reflect rule activation strength rather than probabilistic uncertainty, which may limit their utility in risk-sensitive decision scenarios. Future work could explore adaptive fuzzy systems or hybrid neuro-fuzzy models that learn from new data, thereby reducing dependency on initial expert knowledge. Additionally, expanding the detected classes to include stress indicators (e.g., disease spots, nutrient deficiencies) would increase the system's diagnostic scope but would also necessitate more complex rule bases and additional annotated datasets.

4.5 Practical deployment considerations

The successful edge deployment on NVIDIA Jetson Nano hardware confirms the framework's feasibility for real-time monitoring. However, scaling to larger farms with dozens of cameras would require optimization of communication bandwidth, energy efficiency, and cloud integration. Moreover, the system's effectiveness ultimately depends on farmer acceptance, which hinges on interface design, alert relevance, and ease of integration into existing management practices. Future studies should include user trials to evaluate the practical impact of the generated alerts on decision-making efficiency, labor reduction, and yield outcomes.

5 Conclusions

This study presented the YOLOv7-Fuzzy framework, a hybrid system designed to bridge the gap between low-level visual perception and high-level agronomic decision-making for cantaloupe cultivation. The framework successfully combined the strengths of a state-of-the-art deep learning detector, YOLOv7, with the uncertainty-modeling capabilities of a Mamdani-type fuzzy inference system. Comprehensive evaluation demonstrated that YOLOv7 provided the most stable and accurate detection backbone compared to other YOLO variants, achieving a balanced mAP@0.5 of 0.771 under challenging greenhouse conditions characterized by occlusion, illumination variance, and significant class imbalance.

The core contribution lies in the fuzzy reasoning layer, which was formulated using canonical growth trends derived from eleven cultivation cycles across three distinct farms. This layer effectively mitigated the inherent noise and temporal fluctuations of per-frame detections by interpreting aggregated class counts within their phenological context. The result was a transformation of unstable numerical outputs into interpretable, actionable decisions such as "Check Flower" or "Abnormal Condition," each accompanied by a confidence measure.

The real-world validation, via edge deployment on a Jetson Nano, confirmed the system's practical utility. It autonomously generated alerts that mirrored expert agronomic logic, such as flagging a reversed flower-to-fruit ratio in week 5 or detecting an insufficient wilted-leaf count during late-stage maturation—a key indicator for fruit sweetness development. This demonstrates a move from passive monitoring to active, prescriptive decision support.

In conclusion, the YOLOv7-Fuzzy framework offers a significant step towards automated, intelligent crop management. It provides a robust methodology to handle the visual and temporal uncertainties of real agriculture, delivering interpretable insights that can reduce labor costs, enable timely interventions, and ultimately improve yield quality. Future work will focus on expanding the fuzzy rule base to incorporate additional stressors (e.g., disease symptoms), integrating weather data, and exploring adaptive learning mechanisms for the fuzzy system to personalize recommendations for different cultivars and farm microclimates.

Acknowledgments

The authors express their appreciation to Mbeya University of Science and Technology for providing financial support through the HEET Project fund to facilitate this research and Universiti Teknologi Malaysia through research funds, Vote No. R.J130000.7723.4J626 and R.J130000.7323.4J686

Declarations

Funding

This research was supported by Mbeya University of Science and Technology through the HEET Project fund and by Universiti Teknologi Malaysia under research grants Vote No. R.J130000.7723.4J626 and R.J130000.7323.4J686.

Competing interests

The authors declare that they have no financial or non-financial competing interests that are relevant to the content of this article.

Ethics approval

Not applicable. This study did not involve human participants, animals, or any clinical or biological experiments requiring ethical approval.

Consent to participate

Not applicable.

Consent to publish

Not applicable.

Author contributions

S.L.M. (Sikudhan Lucas Mpuhus) contributed to conceptualization, methodology, software development, data curation, formal analysis, investigation, model training and evaluation, fuzzy system design, visualization, writing of the original draft, and project administration.

M.S.Z.A. (Mohamad Shukri Zainal Abidin) contributed to conceptualization, supervision, methodology refinement, validation, and critical review and editing of the manuscript.

M.S.N. (Mohd Shahkhirat bin Norizan) contributed to data acquisition, annotation support, experimental validation, and review and editing.

M.S.A.R. (Muhammad Shahrul Azwan bin Ramli) contributed to data collection, experimental setup, and technical validation.

K.K.K. (Keshinro Kazeem Kolawole) contributed to data analysis support, visualization assistance, and manuscript review.

R.A.A. (Rizqi Andry Ardiansyah) contributed to literature review, dataset organization, and experimental support.

K.J. (Kasirye Joshua) contributed to literature review, data interpretation, and manuscript proofreading. All authors reviewed and approved the final manuscript.

Data availability

The datasets generated and analyzed during the current study, comprising 2,626 images for YOLOv7 training and 785 images for fuzzy reasoning development, are not publicly available due to institutional and project-related restrictions but are available from the corresponding author on reasonable request.

REFERENCES

1. Ou J, Zhang R, Li X. Research and Explainable Analysis of a Real-Time Passion Fruit Detection Model Based on FSOne-YOLOv7. agronomy. 2023;
2. Wan S, Goudos S. Faster R-CNN for multi-class fruit detection using a robotic vision system. Comput Networks [Internet]. 2020;168:107036. Available from: https://doi.org/10.1016/j.comnet.2019.107036
3. Hu C, Shi Z, Wei H, Hu X, Xie Y, Li P. Automatic detection of pecan fruits based on Faster RCNN with FPN in orchard. Int J Agric Biol Eng. 2022;15(6):189–96.
4. Basri H, Syarif I, Sukaridhoto S, Falah MF. Intelligent System for Automatic Classification of Fruit Defect Using Faster Region-Based Convolutional Neural Network (Faster R-Cnn). Kursor. 2019;10(1):1–12.
5. Altin C. Kiwi Fruit Detection with Deep Learning Methods. Int J Adv Nat Sci Eng Res. 2023;(August).
6. Leibe B, Hutchison D. Computer Vision – ECCV 2016. Springer; 2016.
7. He K, Sun J. Deep Residual Learning for Image Recognition. :1–9.
8. Jadhav VS. Development and Advancement in Image Processing Technique for Detection of Various Diseases in Fruit & Vegetable Plants : A Review. 2021;10(2):31–8.
9. H JYwZsYlRhZs. Detecting endosperm cracks in soaked maize using μCT technology and R-YOLOv7-tiny.pdf. 2023.
10. Tian Y, Yang G, Wang Z, Wang H, Li E, Liang Z. Apple detection during di ff erent growth stages in orchards using the improved YOLO-V3 model. 2019;157(October 2018):417–26.
11. Villacrés J, Viscaino M, Delpiano J, Vougioukas S, Auat F. Apple orchard production estimation using deep learning strategies : A comparison of tracking-by-detection algorithms. Comput Electron Agric [Internet]. 2023;204(March 2022):107513. Available from: https://doi.org/10.1016/j.compag.2022.107513
12. Lawal MO. Tomato detection based on modified YOLOv3 framework. Sci Rep [Internet]. 2021;1–12. Available from: https://doi.org/10.1038/s41598-021-81216-5

13. Environment N. YOLO-Banana : A Lightweight Neural Network for Rapid Detection of Banana Bunches and Stalks in the Natural Environment. 2022;
14. Xiao B, Nguyen M, Qi W. Fruit ripeness identification using YOLOv8 model. Multimed Tools Appl [Internet]. 2023;(June). Available from: https://doi.org/10.1007/s11042-023-16570-9
15. Liu G, Nouaze JC, Lyonel P, Mbouembe T, Kim JH. YOLO-Tomato : A Robust Algorithm for Tomato Detection Based on YOLOv3. 2020;1–20.
16. Mirhaji H, Soleymani M, Asakereh A, Abdanan S. Fruit detection and load estimation of an orange orchard using the YOLO models through simple approaches in different imaging and illumination conditions. Comput Electron Agric [Internet]. 2021;191(November):106533. Available from: https://doi.org/10.1016/j.compag.2021.106533
17. Damdoo R, Kalyani K. Fruit Detection and Three-Stage Maturity Grading Using CNN Fruit Detection and Three-Stage Maturity Grading Using CNN. 2023;(June).
18. Kim E, Hong SJ, Kim SY, Lee CH, Kim S, Kim HJ, et al. OPEN CNN - based object detection and growth estimation of plum fruit (Prunus mume) using RGB and depth imaging techniques. Sci Rep [Internet]. 2022;1–17. Available from: https://doi.org/10.1038/s41598-022-25260-9
19. Chen J, Ma B, Ji C, Zhang J, Feng Q, Liu X. Apple inflorescence recognition of phenology stage in complex background based on improved YOLOv7. Comput Electron Agric [Internet]. 2023;211(June):108048. Available from: https://doi.org/10.1016/j.compag.2023.108048
20. Wang J, Liu M, Du Y, Zhao M, Jia H, Guo Z, et al. PG-YOLO: An efficient detection algorithm for pomegranate before fruit thinning. Eng Appl Artif Intell [Internet]. 2024;134(May):108700. Available from: https://doi.org/10.1016/j.engappai.2024.108700
21. Rodr, iguez-Álvarez JL, Garc, ia-Alcaraz JL, i Vidal RP, Cuevas-Jacques R, D, iaz-Reza JR. Noninvasive system for weight estimation in cactus crops: A YOLOv5-decision tree approach based on interval type-2 fuzzy sets. Chemom Intell Lab Syst. 2024;245:105064.
22. Wang S, Ma K. Analysis and Detection of Orange Images Based on Improved Faster R-CNN Algorithm and Feature Data Analysis. 2023 IEEE 3rd Int Conf Electron Commun Internet Things Big Data. 2023;109–13.
23. Du X, Cheng H, Ma Z, Lu W, Wang M. DSW-YOLO : A detection method for ground-planted strawberry fruits under different occlusion levels. Comput Electron Agric

[Internet]. 2023;214(June):108304. Available from: https://doi.org/10.1016/j.compag.2023.108304

24. Sa I, Ge Z, Dayoub F, Upcroft B, Perez T, Mccool C. DeepFruits : A Fruit Detection System Using Deep Neural Networks. 2016;

25. Maheswari P, Raja P, Apolo-apolo OE, Filippo S, Gennaro D. Intelligent Fruit Yield Estimation for Orchards Using Deep Learning Based Semantic Segmentation Techniques — A Review. Front Plant Sci |. 2021;12(June):1–18.

26. Hu J, Fan C, Wang Z, Ruan J, Wu S. Fruit Detection and Counting in Apple Orchards Based on Improved Yolov7 and Multi-Object Tracking Methods. Sensors. 2023;23(13).

27. Nan Y, Zhang H, Zeng Y, Zheng J, Ge Y. Intelligent detection of Multi-Class pitaya fruits in target picking row based on WGB-YOLO network. Comput Electron Agric [Internet]. 2023;208(March):107780. Available from: https://doi.org/10.1016/j.compag.2023.107780

28. Sneha N, Sundaram M, Ranjan R. Acre-Scale Grape Bunch Detection and Predict Grape Harvest Using YOLO Deep Learning Network. SN Comput Sci [Internet]. 2024;5(2). Available from: https://doi.org/10.1007/s42979-023-02572-9

29. Pinheiro I, Moreira G, Queirós da Silva D, Magalhães S, Valente A, Moura Oliveira P, et al. Deep Learning YOLO-Based Solution for Grape Bunch Detection and Assessment of Biophysical Lesions. Agronomy. 2023;13(4):1–23.

30. Qiu RZ, Chen SP, Chi MX, Wang RB, Huang T, Fan GC, et al. An automatic identification system for citrus greening disease (Huanglongbing) using a YOLO convolutional neural network. Front Plant Sci. 2022;13(December):1–16.

31. Lawal OM. Real-time cucurbit fruit detection in greenhouse using improved YOLO series algorithm. Precis Agric [Internet]. 2024;25(1):347–59. Available from: https://doi.org/10.1007/s11119-023-10074-0

32. Sawant K, Shirwaikar RD, Ugavekar RR, Chodankar CS, Tirodkar BN, Padolkar A, et al. Fruit Identification using YOLO v8 and Faster R-CNN –A Commparative Study. In: 2024 International Conference on Distributed Computing and Optimization Techniques (ICDCOT). 2024. p. 1–6.

33. Safari Y, Nakatumba-Nabende J, Nakasi R, Nakibuule R. A Review on Automated Detection and Assessment of Fruit Damage Using Machine Learning. IEEE Access. 2024;12:21358–81.

34. Corceiro A, Alibabaei K, Assunção E, Gaspar PD, Pereira N. Methods for Detecting and

Classifying Weeds, Diseases and Fruits Using AI to Improve the Sustainability of Agricultural Crops: A Review. Processes. 2023;11(4).

35. Junos MH, Mohd Khairuddin AS, Thannirmalai S, Dahari M. An optimized YOLO-based object detection model for crop harvesting system. IET Image Process. 2021;15(9):2112–25.

36. Wu Z, Wang X, Jia M, Liu M, Sun C, Wu C, et al. Dense object detection methods in RAW UAV imagery based on YOLOv8. Sci Rep [Internet]. 2024;1–23. Available from: https://doi.org/10.1038/s41598-024-69106-y

37. Huang Y, Huang H, Qin F, Chen Y, Zou J, Liu B, et al. YOLO-IAPs: A Rapid Detection Method for Invasive Alien Plants in the Wild Based on Improved YOLOv9. Agric. 2024;14(12).

38. Song J, Zhang Y, Lin S, Han H. TLDDM : An Enhanced Tea Leaf Pest and Disease Detection Model Based on YOLOv8. 2025;1:1–20.

39. Lu D, Wang Y. MAR-YOLOv9: A multi-dataset object detection method for agricultural fields based on YOLOv9. PLoS One [Internet]. 2024;19(10 October):1–22. Available from: http://dx.doi.org/10.1371/journal.pone.0307643

40. Shaik AB, Kandula AK, Tirumalasetti GK, Yendluri B, Kalluri HK. Comparative Analysis of YOLOv11 and YOLOv12 for Automated Weed Detection in Precision Agriculture. Proc 5th Int Conf Pervasive Comput Soc Networking, ICPCSN 2025. 2025;787–93.

41. Huang Y, Liu Z, Zhao H, Tang C, Liu B, Li Z, et al. YOLO-YSTs: An Improved YOLOv10n-Based Method for Real-Time Field Pest Detection. Agronomy. 2025;15(3):1–19.

42. S PK, K NK. Smart Agricultural Technology Drone-based apple detection : Finding the depth of apples using YOLOv7 architecture with multi-head attention mechanism. Smart Agric Technol [Internet]. 2023;5(June):100311. Available from: https://doi.org/10.1016/j.atech.2023.100311

43. Wang CY, Bochkovskiy A, Liao HYM. YOLOv7+appendix. 2022;1–17. Available from: http://arxiv.org/abs/2207.02696

44. Lai Y, Ma R, Chen Y, Wan T, Jiao R, He H. A Pineapple Target Detection Method in a Field Environment Based on Improved YOLOv7. Appl Sci. 2023;13(4).

45. Vaidya S. Leveraging YOLOv7 for Plant Disease Detection. 2023 4th Int Conf Innov Trends Inf Technol. 2023;1–6.

46. Du X, Cheng H, Ma Z, Lu W, Wang M, Meng Z, et al. DSW-YOLO: A detection method

for ground-planted strawberry fruits under different occlusion levels. Comput Electron Agric [Internet]. 2023;214(September):108304. Available from: https://doi.org/10.1016/j.compag.2023.108304

47. Wu D, Jiang S, Zhao E, Liu Y, Zhu H, Wang W, et al. applied sciences Detection of Camellia oleifera Fruit in Complex Scenes by Using YOLOv7 and Data Augmentation. 2022;

48. Liu M, Wang Y, Li X, Han W, Chen W. Multi-task Tomato Fruit and Bunch Maturity Detection Approach Based on Improved YOLOv7. 2023 IEEE 9th Int Conf Cloud Comput Intell Syst. 2023;573–7.

49. Megalingam RK, Manoharan SK, Maruthababu RB. Integrated fuzzy and deep learning model for identification of coconut maturity without human intervention. Neural Comput Appl [Internet]. 2024;36(11):6133–45. Available from: https://doi.org/10.1007/s00521-023-09402-2

50. Tang R, Lei Y, Luo B, Zhang J. YOLOv7-Plum : Advancing Plum Fruit Detection in Natural. 2023;

51. Shao D, Liu Y, Liu G, Wang N, Chen P, Yu J, et al. YOLOv7scb : A Small-Target Object Detection Method for Fire Smoke Inspection. 2025;1–21.

52. Gu Z, He D, Huang J, Chen J, Wu X, Huang B. Simultaneous detection of fruits and fruiting stems in mango using improved YOLOv8 model deployed by edge device. Comput Electron Agric [Internet]. 2024;227(P1):109512. Available from: https://doi.org/10.1016/j.compag.2024.109512

53. Gomroki M, Hasanlou M, Chanussot J. Model based on Encoder-Decoder Network using. IEEE J Sel Top Appl Earth Obs Remote Sens. 2023;PP:1–15.

54. Soeb JA, Jubayer F, Tarin TA, Rashed M, Mamun A, Ruhad FM, et al. Tea leaf disease detection and identification based on YOLOv7 (YOLO - T). Sci Rep [Internet]. 2023;7:1–16. Available from: https://doi.org/10.1038/s41598-023-33270-4

55. Du W, Jia Z, Sui S, Liu P. Table grape inflorescence detection and clamping point localisation based on channel pruned YOLOV7-TP. Biosyst Eng [Internet]. 2023;235:100–15. Available from: https://doi.org/10.1016/j.biosystemseng.2023.09.014

56. Marimin, Mushthofa. Fuzzy Logic Systems and Applications in Agro-industrial Engineering and Technology. 2nd Int Conf Adapt Intell Agroindustry. 2013;(September 2013):233–41.

57. Suksawat B, Komkum P. Pineapple quality grading using image processing and fuzzy

logic based on Thai Agriculture Standards. Proc - 2015 Int Conf Control Autom Robot ICCAR 2015. 2015;218–22.

58. Naghipour M, Ling LS, Connie T. A Review of AI Techniques in Fruit Detection and Classification: Analyzing Data, Features and AI Models Used in Agricultural Industry. Int J Technol. 2024;15(3):585.

59. Puno JC V., Haban JJI, Alejandrino JD, Bandala AA, Dadios EP. Design of a nutrient film technique hydroponics system with fuzzy logic control. IEEE Reg 10 Annu Int Conf Proceedings/TENCON. 2020;2020-Novem:403–8.

60. Jayalalitha S. I nfluence of Panchagavya on Tomato Y ield in Grow B ags. 2017 IEEE Int Conf Power, Control Signals Instrum Eng. 2017;2104–8.

61. Mushtaq Z, Yaqub A, Jabbar M, Khalid A, Iqbal S, Zeb K, et al. Environment Control System for Livestock Sheds Using Fuzzy Logic Technique. Proc - 2016 3rd Int Conf Inf Sci Control Eng ICISCE 2016. 2016;963–7.

62. Gupta T. Detection of Rice Leaf Diseases by using Fuzzy Logic Application. 2024 IEEE Int Conf Comput Power Commun Technol. 2024;5:1056–9.

63. Sharma S, Kumar R, Pathak BK. Analyzing the Impact of Uncertainties with Fuzzy Logic on Service Composition in Smart Agriculture. 2024 Int Conf Emerg Smart Comput Informatics, ESCI 2024. 2024;3–5.

64. Bakar WA, Sum R. Food & Agribusiness Management (FABM) AGRICULTURE RISK MANAGEMENT : A CASE STUDY ON ROCK MELON FARM IN. 2020;1(2):75–82.

65. Fauzie M, Halimatun T, Abu T, Adila F. A Scoping Review of Melon Manis Terengganu Research Perspective in Malaysia. 2022;13(2):10–27.

66. Campus J. Energy use pattern analysis of rockmelon (Cucumis melo) production in Malaysia: a case study. 2020;4(2006):34–9.

67. Cucumis H cooled R. Universiti putra malaysia. 2018;

68. Buah-buahan ST. Statistik tanaman buah-buahan. 2021;

69. Jing X, Wang Y, Li D, Pan W. Melon ripeness detection by an improved object detection algorithm for resource constrained environments. Plant Methods [Internet]. 2024;20(1). Available from: https://doi.org/10.1186/s13007-024-01259-3

70. Yoon S, Cho Y, Ahn TI. Melon Fruit Detection and Quality Assessment Using Generative AI-Based Image Data Augmentation. 2024;1–8. Available from: http://arxiv.org/abs/2407.10413

71. Khairul M, Zakaria Z, Hasan S, Latip R, Irawati ID. Rock Melon Crop Yield Prediction

using Supervised Classification Machine Learning on Cloud Computing. 2024;2(2):200–17.

72. Seeds SG 100. Sakata Glamour - 100 seeds | CNC Marketing - Your Preferred Agricultural Inputs Partner [Internet]. Available from: https://cncagri.com/product/sakata-glamour---100-seeds

73. Bushnag A, Chaabane S Ben, Alshmrani M, Abuzneid S. Smart agriculture : IoT-Based smart irrigation with advanced fuzzy logic control. Expert Syst Appl [Internet]. 2026;299(PD):130168. Available from: https://doi.org/10.1016/j.eswa.2025.130168

74. Benzaouia M, Hajji B, Mellit A, Rabhi A. Fuzzy-IoT smart irrigation system for precision scheduling and monitoring. Comput Electron Agric [Internet]. 2023;215(September):108407. Available from: https://doi.org/10.1016/j.compag.2023.108407

75. Aulia S, Suksmono AB, Mengko TR, Alisjahbana B. A Novel Digitized Microscopic Images of ZN- Stained Sputum Smear and Its Classification Based on IUATLD Grades. IEEE Access. 2024;PP:1.

76. Badgujar CM, Poulose A, Gan H. Agricultural object detection with You Only Look Once (YOLO) Algorithm : A bibliometric and systematic literature review. Comput Electron Agric [Internet]. 2024;223(May):109090. Available from: https://doi.org/10.1016/j.compag.2024.109090

77. Lynn Brandenberger, James Shrefler ER and JD. Melon-Production-Hla-6237.Pdf. Oklahoma Coop Ext Serv. 2021;(March):1–8.